



HAL
open science

Interferon-induced Protein-44 and Interferon-induced Protein 44-like restrict replication of Respiratory Syncytial Virus

D C Busse, D. Habgood-Coote, S. Clare, C. Brandt, I. Bassano, M. Kaforou, J. Herberg, M. Levin, Jean-Francois Eleouet, P. Kellam, et al.

► **To cite this version:**

D C Busse, D. Habgood-Coote, S. Clare, C. Brandt, I. Bassano, et al.. Interferon-induced Protein-44 and Interferon-induced Protein 44-like restrict replication of Respiratory Syncytial Virus. 2024. hal-04494657

HAL Id: hal-04494657

<https://hal.uvsq.fr/hal-04494657>

Preprint submitted on 7 Mar 2024

HAL is a multi-disciplinary open access archive for the deposit and dissemination of scientific research documents, whether they are published or not. The documents may come from teaching and research institutions in France or abroad, or from public or private research centers.

L'archive ouverte pluridisciplinaire **HAL**, est destinée au dépôt et à la diffusion de documents scientifiques de niveau recherche, publiés ou non, émanant des établissements d'enseignement et de recherche français ou étrangers, des laboratoires publics ou privés.

1 **Interferon-induced Protein-44 and Interferon-induced Protein 44-like restrict**
2 **replication of Respiratory Syncytial Virus**

3 D. C. Busse¹, D. Habgood-Coote¹, S. Clare², C. Brandt², I. Bassano¹, M. Kaforou¹, J.
4 Herberg¹, M. Levin¹, Jean-Francois Eleouet³, P. Kellam^{1, 4}, J. S. Tregoning¹

5

6 ¹Department of Infectious Disease, Imperial College London, St. Mary's Campus, London,
7 United Kingdom.

8

9 ²Wellcome Trust Sanger Institute, Wellcome Trust Genome Campus, Hinxton, United
10 Kingdom.

11

12 ³Unité De Virologie et Immunologie Moléculaires (UR892), INRA), Université Paris-Saclay,
13 78350 Jouy-en-Josas, France

14

15 ⁴Kymab Ltd, The Bennet Building (B930), Babraham Research Campus, Cambridge, United
16 Kingdom.

17

18 Contact information for corresponding author: john.tregoning@imperial.ac.uk

19

20 Key words: IFI44, restriction factor, innate immunity, RSV, intrinsic immunity

21 Word count main text: 3434

22 Word count abstract: 159

23 Running head: IFI44 and IFI44L restrict RSV

24 **Abstract**

25 Cellular intrinsic immunity, mediated by the expression of an array of interferon-
26 stimulated antiviral genes, is a vital part of host defence. We have previously used a
27 bioinformatic screen to identify two interferon stimulated genes (ISG) with poorly
28 characterised function, Interferon-induced protein 44 (IFI44) and interferon-induced
29 protein 44-like (IFI44L), as potentially being important in Respiratory Syncytial Virus
30 (RSV) infection. Using overexpression systems, CRISPR-Cas9-mediated knockout,
31 and a knockout mouse model we investigated the antiviral capability of these genes
32 in the control of RSV replication. Over-expression of IFI44 or IFI44L was sufficient to
33 restrict RSV infection at an early time post infection. Knocking out these genes in
34 mammalian airway epithelial cells increased levels of infection. Both genes express
35 antiproliferative factors that have no effect on RSV attachment but reduce RSV
36 replication in a minigenome assay. The loss of *Ifi44* was associated with a more
37 severe infection phenotype *in vivo*. These studies demonstrate a function for IFI44
38 and IFI44L in controlling RSV infection.

39 **Importance**

40 RSV infects all children under two years of age, but only a subset of children get
41 severe disease. We hypothesize that susceptibility to severe RSV necessitating
42 hospitalization in children without pre-defined risk factors is in part mediated at the
43 anti-viral gene level. But there is a large array of anti-viral genes, particularly in the
44 ISG family about which the mechanism is poorly understood. Having observed
45 significantly lower levels of IFI44 and IFI44L gene expression in hospitalized children
46 with a confirmed diagnosis of RSV, we dissected the function of these two genes.
47 Through a range of over-expression and knockout studies we show that the genes
48 are anti-viral and anti-proliferative. This study is important because IFI44 and IFI44L
49 are upregulated after a wide range of viral infections and IFI44L can serve as a
50 diagnostic bio-marker of viral infection.

51 **Introduction**

52 Respiratory syncytial virus (RSV) is a major global cause of morbidity in young
53 children and the elderly, representing a significant burden on healthcare
54 infrastructure (1). The majority of RSV infections in susceptible populations are self-
55 limiting, however some 2% of infected infants develop a severe infection and require
56 hospitalisation. The risk factors behind this development of severe RSV disease
57 have yet to be fully elucidated and some 75% of hospitalised infants present with no
58 known risk factor (2, 3). This suggests that there is a genetic element to susceptibility
59 to symptomatic infection and since ISGs are vital in early viral control, they are a
60 likely candidate. A number of ISG have been demonstrated to inhibit RSV including
61 IFITM proteins (4, 5) TDRD7 (6), and 2'-5' oligoadenylate synthetase (7).

62 A vital component of the innate host response to viral infection is the intracellular
63 amplification of an array of antiviral proteins in response to type I interferon (IFN).
64 The majority of these inducible proteins, encoded by IFN-stimulated genes (ISGs),
65 have no defined function and have only been poorly characterised in terms of their
66 antiviral tropism. Understanding how these genes reduce viral infection gives insight
67 into the viral life cycle and may open up novel therapeutic routes. We have
68 previously performed a bioinformatic screen of ISG expressed after RSV infection,
69 which prioritised ISG of interest for further study (8).

70 Two ISGs of interest identified in our previous work are *IFI44* and *IFI44L*, which are
71 found adjacently on chromosome one. *IFI44L* is a larger gene of 26 kilobases (kb)
72 compared to the 14 kb of *IFI44*, but both genes encode similar sized proteins
73 translated from a transcript produced from nine exons. *IFI44* is made up of 444
74 amino acids whereas *IFI44L* has 452 residues: the two proteins share 45% amino

75 acid identity. *IFI44*, previously known as *MTAP44*, was first identified in the context
76 of Hepatitis C virus infection (9, 10). Overexpression of IFI44 has been shown to
77 restrict Bunyamwera virus (11), and HIV-1 (12) infection *in vitro*. IFI44 was initially
78 described as a cytoplasmic protein, however two studies have observed that low
79 levels of IFI44 can be found in the nucleus (12, 13). Hallen *et al.* reported that
80 overexpression of IFI44 was able to reduce proliferation of two melanoma cell lines
81 independently of IFN-I (13). The anti-proliferative mechanism of IFI44 remains
82 unexplored.

83 Even less is known about the tropism and function of IFI44L. IFI44L has been shown
84 to have a moderate impact on Hepatitis C virus infection (14). Interestingly, *IFI44L*
85 expression has also been associated with several autoimmune disorders (15-17),
86 cancer (18, 19), and humoral responses to vaccination (20). These seemingly
87 disparate contexts suggest that *IFI44L* may be a biomarker of IFN responses
88 independent of the type of stimulus. Interestingly, IFI44L expression is sufficient to
89 distinguish viral from bacterial infection (21). Like IFI44, IFI44L has antiproliferative
90 activity, associated with increased activation of Met/Src signalling (18).

91 Using both overexpressing and knockout cell lines, we demonstrated that IFI44 and
92 IFI44L are antiproliferative factors that can independently restrict RSV infection. We
93 report that this ability to restrict infection involves the reduction of viral genome
94 transcription or replication but was not dependent upon a predicted guanosine-5'-
95 triphosphate (GTP)-binding region present in either protein. We demonstrate for the
96 first time that the loss of IFI44 expression in a mouse model of infection is associated
97 with more severe RSV disease.

98 **Methods**

99 **Clinical cohort.** *IFI44* and *IFI44L* expression was analysed in a published clinical
100 cohort of febrile infants with either moderate or severe RSV infection [13]. The
101 microarray gene expression dataset (GSE72810) was retrieved from the National
102 Institutes of Health Gene Expression Omnibus database (22) using the GEOquery
103 package (23) in R (24). Normalisation was performed using robust spline
104 normalisation (RSN) from the lumi package (25) followed by a log transformation.
105 Patients with suspected or confirmed bacterial infection were removed (n = 4).
106 Cohort demographics are described in the associated figures. Prior to differential
107 expression probes were removed if the expression was not above 6 in at least 4
108 samples. Differential expression was performed using Limma and expression values
109 were normalised using robust spline normalisation and a log transformation, plotted
110 p-values are not adjusted for multiple testing (values in tables are Benjamini-
111 Hochberg corrected). Interferon stimulated genes were downloaded from KEGG.

112 **Cell culture and viruses.** HEp-2 (from P. Openshaw, Imperial College London),
113 A549 (ATCC CCL-185), and HEK293T/17 (ATCC CRL-11268) cells were maintained
114 in Dulbecco's modified eagle medium supplemented with 10% v/v foetal calf serum,
115 1% v/v penicillin/streptomycin, and 1% v/v L-glutamine. RSV strain A2 (from P.
116 Openshaw, Imperial College London) and rgRSV (26) were passaged in HEp-2 cells
117 before quantification of viral titre by plaque assay. VSV-G pseudotyped Lentiviral
118 particles were produced by triple transfection in HEK293T/17 cells using
119 Lipofectamine 3000 (Thermofisher). Lentiviral vectors pTRIP-FLUC-tagRFP, pTRIP-
120 IFI44-tagRFP, and pTRIP-IFI44L-tagRFP were a kind gift from M. Dorner (Imperial
121 College London). To generate mutant proteins these vectors were altered by using
122 QuickChange® XL site-directed mutagenesis (Agilent Technologies) according to the

123 manufacturer's instruction. Lentivirus was harvested 24-52 hours after transfection
124 and concentration of transducing units (TU) determined by flow cytometry. For
125 transduction, 5×10^4 cells were seeded into each well of a 24-well plate. After 24
126 hours cells were transduced with 2×10^5 TU ml⁻¹ lentivirus containing supernatant.
127 Stably transduced clonal populations were recovered following fluorescence-
128 activated cell sorting (FACS). RFP expression was monitored over three weeks and
129 expression of IFI44 or IFI44L confirmed by quantitative PCR (qPCR) or Western
130 blotting.

131 **Quantitative PCR.** For analysis of *in vitro* samples, cells were lysed in RLT buffer
132 and RNA extracted using Qiagen RNeasy kit according to the manufacturer's
133 instructions (Qiagen). RSV viral load *in vivo* was assessed by extracting RNA from
134 frozen lung tissue using Trizol extraction after disruption in a TissueLyzer (Qiagen).
135 Complementary DNA (cDNA) was reverse transcribed from RNA extracts using
136 GoScript reverse transcriptase with random primers according to the manufacturer's
137 instructions (Promega). qPCR reactions were carried out on a Stratagene Mx3005p
138 thermal cycler (Agilent Technologies). RSV viral load was quantified by amplification
139 of the RSV L gene using 900 nM forward primer (5'-
140 GAACTCAGTGTAGGTAGAATGTTTGCA-3'), 300 nM reverse primer (5'-
141 TTCAGCTATCATTCTCTGCCAAT-3'), and 100 nM probe (5'-FAM-
142 TTTGAACCTGTCTGAACAT-TAMRA-3') in Taqman™ Universal master mix, no
143 AmpErase™ UNG (Thermofisher). Absolute copy number was calculated by
144 comparison to a plasmid standard. mRNA was amplified with SYBRselect master
145 mix (Thermofisher) according to the manufacturer's instructions. The following
146 primers were used at a final concentration of 250 nM: hIFI44 (forward 5'-
147 TGGTACATGTGGCTTTGCTC-3', reverse 5'-CCACCGAGATGTCAGAAAGAG-3'),

148 hIFI44L (forward 5'-AAGTGGATGATTGCAGTGAG-3', reverse 5'-
149 CTCAATTGCACCAGTTTCCT-3'), hGAPDH (forward 5'-
150 GGACCTGACCTGCCGTCTAG-3', reverse 5'-TAGCCCAGGATGCCCTTGAG-3'),
151 *mIfi44* (forward 5'-AACTGACTGCTCGCAATAATGT-3', reverse 5'-
152 GTAACACAGCAATGCCTCTTGT-3'), *mIfi44l* (forward 5'-
153 AGTGACAGCCAGATTGACATG-3', reverse 5'-CATTGTGGATCCCTGAAGAGAA-
154 3'), and *mGapdh* (forward 5'-AGGTCGGTGTGAACGGATTTG-3', reverse 5'-
155 TGTAGACCATGTAGTTGAGGTCA-3'). Fold-change in target gene in treated
156 samples was calculated using the $\Delta\Delta C_t$ method (Ct = cycle threshold) and
157 normalised to a reference transcript (27).

158 **Western blotting.** Cells were lysed using RIPA buffer (Sigma) containing 1 x
159 cOmplete™ Ultra protease inhibitor cocktail (Sigma). Proteins were separated by
160 SDS-PAGE using 4-20% pre-cast Mini-Protean TGX gels (Bio-rad) before transfer
161 onto a nitrocellulose membrane using the Trans-Blot turbo transfer system (Bio-rad).
162 Membranes were blocked for 1 hour at room temperature (RT) with 5% milk in PBS
163 with 0.1% Tween 20. Membranes were probed using the following primary
164 antibodies for 16 hours at 4°C: IFI44 (ThermoFisher, PA5-65370) and IFI44L (VWR,
165 ARP46166), β -actin (Abcam, ab82227). Membranes were washed and probed with
166 anti-IgG HRP-conjugated antibodies (Dako) prior to chemiluminescent detection.

167 **Flow cytometry.** Analysis was performed on a Becton Dickinson Fortessa LSR
168 using a 561 nm laser and 582/15 band pass filter to detect tag-RFP positive cells, a
169 499 nm laser and 530/30 band pass filter to detect GFP positive cells. Acquisition
170 was set to record 10^4 events followed by doublet gating and analysis with FlowJo
171 V10.

172 **RSV Plaque assay.** RSV titre in cell-free supernatant was quantified by
173 immunoplaque assay using biotinylated goat anti-RSV polyclonal antibody (Abcam).
174 HEp-2 cells were infected with dilutions of RSV-containing supernatant for 24 hours.
175 Cells were fixed in methanol containing 2% hydrogen peroxide for 20 minutes at RT.
176 Cells were washed with 1% bovine serum albumin (BSA) PBS prior to addition of
177 anti-RSV antibody for 1 hour. Plaques were then visualised by incubating the cells
178 with ExtrAvidin peroxidase followed by 3 amino-ethylcarbazole substrate (Sigma).

179 **CRISPR knockout generation.** Guide RNA (gRNA) sequences targeting human
180 *IFI44* (gRNA1: CAA TAC GAA TTC T; gRNA2: GAA AGA AGG CGG CCT GTG C)
181 and *IFI44L* (gRNA1: TAA CCT AGA CGA CAT AAA G; gRNA2: GTG ACT GGC CAA
182 GCC GTA G) were synthesised according to Sanjana et al (28) and cloned into
183 pSpCas9(BB)-2A-GFP (Addgene, #48138) following *BbsI* digestion. Insertion of
184 gRNA sequences validated by sequencing (Eurofins Genomics). A549 cells were
185 transfected and sorted by FACS after 48 hours. Clonal knockouts were validated by
186 PCR amplification of the targeted region, agarose gel electrophoresis, Western
187 blotting, and sequencing. Clustal Omega was used for multiple sequence alignment
188 (29).

189 **Proliferation assays.** Viable cell numbers were quantified either by Trypan blue
190 exclusion or by the production of formazan product (OD^{490}) 2 hours after addition of
191 CellTiter 96[®] Aqueous One Solution assay reagent (Promega) according to the
192 manufacturer's instructions. Different cell lines were seeded at equal densities and
193 viable cell number quantified 6-48 hours later. Cell division was assessed by staining
194 cells with 5 μ M CellTrace Violet reagent (Thermofisher) and flow cytometric analysis
195 (10^4 single cell events, 405 nm laser with a 450/50 band pass filter) after 72 hours.

196 Prior to analysis cells were harvested and fixed for 20 minutes at RT in 4%
197 paraformaldehyde.

198 **RSV cold-bind assay.** Stably transduced cell lines were seeded at equal densities
199 24 hours prior to infection. Each cell line was counted prior to infection to ensure
200 inoculums were normalised across different cell lines. Cells were equilibrated to 4°C
201 for 30 minutes before media was removed and infected with RSV A2 in a minimal
202 volume of serum-free DMEM for 90 minutes at 4°C. Cells were then washed 3 x with
203 ice-cold 1x PBS and lysed in RLT buffer (Qiagen) with 1/100 β-mercaptoethanol
204 (Sigma) for quantification of RSV L gene RNA.

205 **RSV minigenome assay.** The RSV Minigenome and plasmids expressing RSV L,
206 N, P, and M2-1 proteins were described previously (30). pGEM3-Gaussia/Firefly
207 encodes a sub-genomic RSV replicon. From the 3' end: A2 leader sequence (Le),
208 Gaussia luciferase open-reading frame (ORF) with an NS1 gene start (GS) and M
209 gene end (GE) sequence, Firefly luciferase ORF with SH GS and GE sequences, A2
210 trailer region (Tr). HEK293T/17 cells and stably transduced 293T/17 cell lines were
211 seeded 24 hours prior to transfection at 90% confluency in 24-well plates. The cells
212 were transfected using Lipofectamine 3000 with a DNA mixture of 0.25 µg pGEM3-
213 Gaussia/Firefly minigenome, 0.125 µg pCITE-L, 0.25 µg pCITE-P, 0.06 µg pCITE-
214 M2-1, 0.25 µg pCITE-N, 0.12 µg pSV-β-Gal (Promega), and 0.25 µg pCAGGS-T7
215 (Addgene #65974). Negative controls were transfected with the DNA mix with
216 pCITE-L replaced by pcDNA3.1. Cells were lysed in 1 x passive lysis buffer
217 (Promega) after 24 hours. Firefly luciferase activities were measured in 10 µl of
218 lysate using 50 µl luciferase assay substrate (Promega). To normalise transfection
219 efficiencies β-Galactosidase levels were measured using the β-Galactosidase
220 Enzyme Assay System (Promega). 20 µl of lysate was diluted 1:1 in 1x reporter lysis

221 buffer before addition of 40 μ l 2x assay buffer. Following incubation at 37°C for 1
222 hour 150 μ l 1 M Na₂CO₃ was added and absorbance measured at 420 nm.

223 **Mouse infection.** Background-, sex-, and age-matched, >95% C57BL/6N or
224 BALB/c, wild type and *Ifi44*^{tm1b(komp)Wtsi} (*Ifi44*^{-/-}) mice (31) (Wellcome Trust Sanger
225 Institute) were supplied with food and water *ad libitum* and monitored daily. Mice
226 were infected intranasally (i.n.) with 1-4 x 10⁵ plaque-forming units (PFU) of RSV A2
227 in 100 μ L under isoflurane anaesthesia.

228 **Enzyme-linked immunosorbent assay.** Bronchoalveolar lavage fluid (BALF) was
229 collected by inflating the lungs with PBS. Supernatant was collected after
230 centrifugation and assayed. For lung homogenate, lung tissue was homogenised
231 through a 100 μ m cell strainer (Falcon) and supernatant collected after centrifugation
232 and ACK lysis. Cytokines in lung homogenate and BALF were quantified using
233 DuoSet ELISAs according to the manufacturer's instructions (R&D systems).

234 **Luminex[®] multiplex ELISA.** Lung homogenate supernatant was subjected to a
235 magnetic Luminex[®] assay using a premixed multi-analyte kit: CXCL10, CCL3,
236 CXCL2, CXCL1, IL-5, CCL2, IL-1 α , and CCL5 (R&D systems). Samples and diluted
237 microparticles were combined according to the manufacturer's instructions and
238 incubated for 2 hours at RT (800 rpm). A magnet was applied to the bottom of the
239 plate and wells were washed x 3 for 1 minute each, before addition of a Biotin
240 Antibody cocktail (1h RT, 800 rpm). The previous wash was repeated, and
241 Streptavidin-PE added to each well (30m RT, 800 rpm). The wash was repeated and
242 microparticles resuspended in wash buffer for analysis on a Bio-Plex[®]100 Luminex
243 machine (Bio-rad).

244 **Statistical analysis.** Analysis performed in Prism 8 as described in figure legends
245 (GraphPad Software).

246 **Ethics.** All animal experiments were maintained in accordance with UK Home Office
247 regulations, the UK Animals (Scientific Procedures) Act 1986 and reviewed by an
248 Animal Welfare and Ethical Review Body. The work was done under PPL
249 P4EE85DED. Clinical data presented was collected in a previous study [13]. Written
250 informed consent was obtained from parents or guardians using locally approved
251 research ethics committee permissions (St Mary's Research Ethics Committee (REC
252 09/H0712/58 and EC3263); Ethical Committee of Clinical Investigation of Galicia
253 (CEIC ref 2010/015); UCSD Human Research Protection Program No. 140220; and
254 Academic Medical Centre, University of Amsterdam (NL41846.018.12 and
255 NL34230.018.10).

256 **Results**

257 **IFI44 and IFI44L expression in human infants with severe RSV infection**

258 We have previously identified a number of ISGs that are consistently upregulated in
259 response to RSV (8), of which IFI44 and IFI44L featured prominently. We focussed
260 on these two genes as relatively little was known of their phenotype. Our hypothesis
261 was that at an individual gene level, there should be a significant difference in gene
262 expression RSV infected children with severe disease. To test this, we examined
263 gene expression levels of both *IFI44* and *IFI44L* in data previously generated by
264 microarray on RNA extracted from whole blood derived PBMCs, collected from
265 children with confirmed RSV infection. We compared those who required paediatric
266 intensive care unit (PICU) admission with those who were admitted to a general
267 hospital ward (General). When investigated as individual genes in the dataset, the
268 expression of both IFI44 ($P = 0.0082$, Fig. 1b) and IFI44L ($P = 0.0248$, Fig. 1c) was
269 significantly lower in those patients admitted to the paediatric intensive care unit
270 (PICU). IFI44 expression correlated with IFI44L expression across both moderate
271 and severe RSV patients ($p < 0.001$, $r^2 = 0.74$, Fig. 1d). It should be noted that, when
272 investigated in the context of global gene expression data, the differences between
273 general hospital and intensive care admission were not significant, though IFI44L did
274 have a greater than 2log fold change (Fig. 1e). This observed difference supported
275 the rationale for looking at the function of IFI44 and IFI44L in more detail.

276 ***IFI44* and *IFI44L* are upregulated early in response to IFN-I and RSV**

277 Human lung epithelial A549 cells treated with recombinant IFN α 2a robustly
278 upregulated expression of *IFI44* and *IFI44L* mRNA within 2 and 6 hours respectively
279 ($P < 0.01$, Fig. 2a). Induction following RSV infection was slower than IFN, with *IFI44*

280 and *IFI44L* upregulated within 6 and 12 hours ($P < 0.05$, Fig. 2b). Expression
281 remained upregulated for at least 48 hours following treatment or infection. IFI44
282 protein was increased following 24-48 hours of IFN α 2a stimulation (Fig. 2c) and
283 undetectable in unstimulated cells. IFI44L protein was detectable in unstimulated
284 cells, it did not appear to be induced by IFN treatment relative to the control
285 untreated cells (Fig. 2c). After recombinant IFN treatment expression of both genes
286 plateaued after 6 hours but expression continued to increase during the first 48
287 hours of RSV infection, in parallel with viral RNA levels (Fig. 2d). When cells were
288 pre-treated with IFN α 2a before infection, there was a significant reduction in viral
289 RNA levels (Fig. 2e)

290 Similarly, the expression of both *Ifi44* and *Ifi44l* RNA was significantly upregulated
291 rapidly after intranasal infection of BALB/c mice, detectable from 6 hours ($P < 0.05$,
292 Fig. 2f). Gene expression peaked after 24 hours and returned towards baseline
293 levels by day 14 in parallel with levels of viral RNA that also reduced as the infection
294 was cleared (Fig. 2g).

295 **Overexpression of IFI44 or IFI44L restricts RSV infection**

296 In a previous screen to identify ISGs that impact RSV infection McDonald *et al.*
297 showed that transient overexpression of human IFI44 or IFI44L by lentiviral
298 transduction reduced the percentage of RSV infected cells (8). Here, we generated
299 stably transduced clonal cell lines by lentiviral transduction, followed by
300 fluorescence-activated cell sorting (FACS) selection. Following expansion, clonal
301 populations were selected that expressed TagRFP after three weeks in culture
302 following sorting. Individual cell lines were then selected based on detectable
303 expression of either *IFI44* or *IFI44L* by qPCR (Fig. 3a). *MX1* expression was

304 assessed in each stable cell line to confirm the specificity of overexpression to either
305 *IFI44* or *IFI44L*. There were no significant differences in expression of *MX1* in either
306 cell line following IFN-I stimulation suggesting that neither *IFI44* or *IFI44L* are
307 regulators of the IFN response.

308 To monitor the impact on infection, cells were infected with m.o.i. 0.1 or 0.01
309 recombinant GFP-expressing RSV (rgRSV), and the percentage of RFP⁺ single cells
310 that were GFP⁺ was quantified after 24 hours. After 24 hours of rgRSV infection, cell
311 lines expressing either *IFI44* or *IFI44L* showed a significant reduction in the
312 percentage of infected cells relative to cells stably transduced with empty vector ($P <$
313 0.05 , Fig. 3c). To confirm the impact on RSV infection we examined the impact on
314 wild-type RSV A2 infection in these stable cell lines. We observed a significant
315 reduction in viral RNA 24 hours after infection (m.o.i. 0.01) ($P < 0.05$, Fig. 3d). To
316 observe impact on virus progeny production, we measured the viral titre 48 hours
317 after infection. The recoverable titre of RSV A2 virus was significantly reduced in
318 cells expressing either *IFI44* or *IFI44L* ($P < 0.05$, Fig. 3e).

319 In order to demonstrate that the impact of *IFI44* expression is not a result of clonal
320 differences, we transduced polyclonal A549 cells with lentivirus expressing either
321 Firefly luciferase (FLUC) or *IFI44* and subsequently infected the cells with rgRSV
322 after 24 hours. Expression of *IFI44* protein was confirmed (Fig. 3f) and significant
323 restriction in rgRSV infection ($P < 0.05$, Fig. 3g) was observed similar to that seen in
324 the stably transduced cell line. Overall these data suggest that both *IFI44* and *IFI44L*
325 are able to restrict RSV infection.

326 **Knockout of *IFI44* results in elevated RSV infection *in vitro***

327 To further examine the role of IFI44 or IFI44L on RSV infection we used a pool of
328 endoribonuclease-prepared siRNA (esiRNA) targeting *IFI44* to knockdown
329 expression. These esiRNAs reduced levels of *IFI44* mRNA by only 48% ($P < 0.01$)
330 and also reduced *IFI44L* mRNA levels by 30%, although this was not statistically
331 significant (Fig. 4a). However, esiRNA knockdown was sufficient to cause an over 2-
332 fold increase in the levels of viral RNA in esiRNA-IFI44 transfected A549 cells
333 infected with RSV A2 (m.o.i. 0.1) relative to cells transfected with a non-targeting
334 control ($P < 0.01$, Fig. 4b).

335 Due to the low efficiency of the knockdown and potential unintended impact of siRNA
336 on *IFI44L* expression we developed CRISPR-Cas9 edited IFI44 and IFI44L deficient
337 cell lines, this also enabled us to investigate the impact of double knockouts. A549
338 cells were transfected with two guide RNA (gRNA) constructs encoded *in cis* with the
339 *Streptococcus pyogenes* Cas9 enzyme and a GFP marker. gRNA sequences
340 targeting regions in exons 4 and 5 of *IFI44* and exons 3 and 4 of *IFI44L* were used.
341 Following transfection, the top 2% GFP⁺ cells were sorted as single cells. Gene
342 editing was confirmed in clonal populations through PCR of the targeted region (data
343 not shown) and loss of either IFI44 or IFI44L protein expression after treating with
344 IFN α (Fig. 4c). Five IFI44 deficient (Δ IFI44), two IFI44L deficient (Δ IFI44L), and three
345 clonal populations deficient in both IFI44 and IFI44L (Δ IFI44 Δ IFI44L) were isolated.
346 Selection of clones was based on sequencing. The Δ IFI44 clone selected for further
347 study had mutations resulting in a frameshift and stop codon formation in each
348 detectable allele. The Δ IFI44L clone selected had a large deletion in one allele and
349 disruption of an exon-intron boundary.

350 The selected clones were treated with 500 IU ml⁻¹ IFN α 2 α and subsequently infected
351 with RSV A2 for 24 hours (Fig. 4d). There were significantly increased levels of viral

352 RNA in the $\Delta IFI44$ clone at m.o.i. 0.1 ($P < 0.01$), although we noted a non-significant
353 increase in infection in the $\Delta IFI44\Delta IFI44L$ cells ($P = 0.079$). The loss of *IFI44L*
354 expression was only associated with a significant increase in viral RNA at m.o.i. 0.01
355 ($P < 0.01$). Clones were infected with RSV A2 (m.o.i. 0.1) for 48 hours and viral titre
356 assessed in the culture medium, there was with a >2-fold increase in viral titre (Fig.
357 4e) in each clone. Knockout of both *IFI44* and *IFI44L* resulted in a 4-fold increase in
358 viral titre (Fig. 4e, $P < 0.05$).

359 ***IFI44* and *IFI44L* reduce cellular proliferation**

360 Previous studies have described an effect of *IFI44* or *IFI44L* on cell proliferation (13,
361 18). We investigated the impact of these factors on proliferation by assaying growth
362 of selected knockout clones. Knocking out either or both genes was associated with
363 increased proliferation, using a colorimetric assay measuring cellular metabolic
364 activity ($P < 0.05$, Fig. 5a). When viable cell numbers were quantified manually by
365 Trypan blue exclusion only the *IFI44* KO was associated with a significant increase
366 in cell number ($P < 0.05$, Fig. 5b). Overexpression of either gene led to a significant
367 reduction in proliferation after 24 hours quantified by either method ($P < 0.05$, Fig.
368 5c-d). Cells perfused with CellTrace Violet dye were allowed to proliferate for 72
369 hours prior to analysis by flow cytometry to assess cell division. We noted that both
370 *IFI44* and *IFI44L* stably transduced cell lines had an increased mean fluorescence
371 intensity ($P < 0.05$, Fig. 5f) suggesting reduced dye dilution and a reduced rate of cell
372 division. The overexpression of *IFI44* or *IFI44L* was not associated with any increase
373 in cytotoxicity, further suggesting that the observed reduction in viable cell number
374 and proliferation is not a result of increased cell death (Fig. 5g).

375 ***IFI44* reduces RSV polymerase activity**

376 To investigate where in the viral life cycle IFI44 and IFI44L have an impact we
377 analysed infection at an acute time point (8h) where viral positive cells should only
378 be newly infected cells and not the result of cell-cell virus spread. IFI44 or IFI44L
379 expression reduced the percentage of infected cells by 44% ($P < 0.01$) and 34%
380 ($P = 0.11$) respectively (Fig. 6a-b) relative to vector control cells, suggesting both
381 proteins are impacting a stage of the viral life cycle prior to new virion release. Using
382 a cold-bind infection assay (RSV A2, m.o.i. 2), where the virus is able to bind the cell
383 surface but is not internalised, we saw no significant difference in levels of viral RNA
384 between cell lines expressing either FLUC (Vector), IFI44, or IFI44L (Fig. 6c). To
385 bypass cell entry and to assess whether IFI44 or IFI44L restrict RSV genome
386 replication or transcription we transfected stably transduced clonal 293T cells with an
387 RSV minigenome system. IFI44 expression reduced minigenome activity by 44%
388 ($P < 0.05$), suggesting reduced RSV polymerase activity (Fig. 6d). The stably
389 transduced 293T line expressing IFI44L also reduced minigenome activity by 45%
390 although this was not statistically significant ($P = 0.085$).

391 **A predicted GDP/GTP-binding site in IFI44 is dispensable for antiviral activity**

392 IFI44 and IFI44L both contain predicted GTPase regions. Five motifs, G1-G5, are
393 involved in GTP hydrolysis and the required nucleotide and cofactor interactions
394 (32). Both proteins contain a putative G1 region (GXXXXGKS), initially identified in
395 IFI44 by Hallen *et al* (13), that is predicted to bind the β -phosphate of GDP or GTP
396 (32). The terminal serine residue also contributes to Mg^{2+} binding. The G1-G4
397 regions of human IFI44 and IFI44L were recently annotated by McDowell *et al* (Fig.
398 6e) (33). The G3 DxxG motif in IFI44 and IFI44L is immediately followed by a
399 hydrophobic leucine residue found in other dynamin-like GTPases such as GBP1,
400 instead of a catalytic glutamine residue seen in ras-like GTPases. IFI44L also

401 contains a G4 motif which mediates binding to the guanine base of GDP or GTP.
402 However, IFI44 does not contain a complete G4 motif. G5 residues are not easily
403 recognised as they are not as well conserved as G1-4 motifs.

404 A549 WT cells were transduced with a lentivirus expressing FLUC (Vector), IFI44
405 WT, or IFI44 $\Delta_{193-201}$ with the G1 region deleted. Mutation of this region in another
406 IFN-inducible GTPase, GBP1, has been shown to reduce nucleotide binding around
407 up to 50-fold, having a greater impact than mutation of G2-G4 regions (34). A
408 comparable reduction in rgRSV infectivity was seen in cells transduced with either
409 IFI44 $\Delta_{193-201}$ or IF44 WT (Fig. 6f), suggesting this region is not required for its antiviral
410 function.

411 **Disease severity is altered in an *Ifi44*^{-/-}/*Ifi44L*^{-/-} mouse model of RSV infection**

412 Having demonstrated that IFI44 and IFI44L were able to impact RSV infection *in vitro*
413 we then investigated the effect of the absence of *Ifi44* and *Ifi44L* in an *in vivo* mouse
414 model of RSV infection. The wild-type C57BL/6N used in this study are *Ifi44L*^{-/-},
415 presumably as a result of gene loss over colony in-breeding, so the comparison was
416 between IFI44^{-/-}/IFI44L^{-/-} and IFI44^{+/+}/IFI44L^{-/-} (WT). Age-matched *Ifi44*^{-/-} and WT
417 mice were infected intranasally with 10⁵ PFU RSV A2 and monitored for weight
418 change over a 7-day infection. Animals were sacrificed at day 4 and 7 after infection.
419 There was greater weight loss in *Ifi44*^{-/-} mice than wild-type controls from days 5-7
420 after infection (P < 0.01, Fig. 7a). There was no difference in total cell numbers
421 isolated from the bronchoalveolar lavage fluid or from whole lung tissue (Fig. 7b-c).
422 Levels of viral RNA in lung tissue was also significantly higher in *Ifi44*^{-/-} mice at day 4
423 (P < 0.01) but not at day 7 (Fig. 7d).

424 Levels of inflammatory cytokines and immunomodulatory factors were analysed
425 either by ELISA or Luminex. Here we noted that most measured analytes (IL-6,
426 CCL3, CXCL2, CXCL1, CCL2, IL-5, IL-1 α , and CCL5) were not significantly different
427 between the WT and *Ifi44*^{-/-} groups (Fig. 7e-f). CXCL10 (P < 0.05, Fig. 7f) and IL-1 β
428 (P < 0.05, Fig. 7e) were both significantly but modestly reduced in the KO animals on
429 day 4 after infection. There was no difference in any measured cytokine on day 7
430 after infection (Fig. 7g) To determine whether the lack of IFI44 modulated IFN
431 responses to RSV infection both *Ifn*- β and *Ifn*- γ expression was assessed by qPCR.
432 Both wild-type and *Ifi44*^{-/-} groups demonstrated similar levels of *Ifn*- β (Fig. 7h) and
433 *Ifn*- γ (Fig. 7i) mRNA.

434 **Discussion**

435 The data presented here explore how the ISGs IFI44 and IFI44L modulate viral
436 infection. We demonstrate that IFI44 and IFI44L restrict RSV infection and reduce
437 RSV genome replication or transcription. We also show, for the first time, that RSV
438 infection is enhanced in an *Ifi44*^{-/-}/*Ifi44L*^{-/-} knockout mouse model. Infectivity was
439 reduced by IFI44 expression at just 8 hours after infection, suggesting restriction of
440 infection occurs before the exit of new virions. Virus attachment was unaffected by
441 either IFI44 or IFI44L expression, this was expected as these proteins are both
442 predicted to be internally expressed (12, 13). Using an RSV minigenome assay, we
443 found that IFI44 expression significantly reduced RSV polymerase activity. However,
444 we cannot say whether this is an impact specifically on the replication or transcription
445 of the viral genome. We also observed that both IFI44 proteins decreased the rate of
446 cellular proliferation. Reduced proliferation is a common feature of the IFN response,
447 mediated by canonical ISGs such as protein kinase R (PKR) (35) and the IFN-
448 induced tetratricopeptide repeat (IFIT) family (36). Whether the anti-proliferative
449 function of the IFI44 proteins is a causative mechanism of their antiviral activity is not
450 clear, because cell cycle arrest may increase the availability of cellular machinery
451 required for replication and virus assembly (37). For example, the RSV matrix protein
452 (M) has previously been shown to induce cell cycle arrest by inducing p53/p21
453 expression in alveolar epithelial cells, enhancing infection (38, 39). The two genes
454 have a high degree of homology and whether they have distinct mechanisms or are
455 redundant is unclear at this time.

456 Our *in vitro* studies have some limitations, primarily the use of clonal cell lines to
457 assay infection and proliferation. We note that transduction of polyclonal parental
458 A549 cells with IFI44 is capable of restricting RSV infection similarly to the stably

459 transduced cells, and that previous studies have observed similar impacts of IFI44
460 on proliferation (13, 18) or restriction of RSV (8). However, it is possible that clone-
461 specific differences have some impact on either RSV infection or cell viability and
462 these data should be interpreted with this limitation in mind. In the knockout cell line,
463 there was a slight difference in the effect on viral RNA and infectious virus
464 recovered, this may reflect differences in the two assays or a difference in where the
465 ISG affect replication or packaging.

466 This is the first study to describe viral infection in *Ifi44*^{-/-}/*Ifi44L*^{-/-} mice. *Ifi44*^{-/-}/*Ifi44L*^{-/-}
467 mice were markedly more susceptible to RSV infection than WT mice, exhibiting
468 increased weight loss and elevated viral load. The genome sequence of C57BL/6N
469 mice reveals a deletion in *Ifi44l* predicted to ablate expression. We were unable to
470 detect transcription of this gene in these mice during RSV infection whereas this was
471 readily detectable in the lungs of RSV-infected BALB/c mice. We observed that *Ifi44*
472 ^{-/-}/*Ifi44L*^{-/-} mice infected with RSV had higher levels of viral RNA present in their lungs
473 at the peak of infection, along with decreased expression of the pro-inflammatory
474 factor IL-1 β . A previous study has noted that in adult mice, blockade of IL-1 β prior to
475 RSV infection, results in elevated viral load (40). Decreased production of this key
476 cytokine along with increased viral replication, due to changes in cellular proliferation
477 and metabolism driven by the loss of IFI44, may go some way to explaining these
478 observations. We saw no change in TNF, but this reflects our recent findings that
479 TNF is only associated with early weight loss after RSV infection, but not later time
480 points (41).

481 Our data showing an antiviral role for IFI44 and IFI44L matches our previous study
482 using a lentivirus screen (8) and a broader screen by another group using the same
483 lentivirus panel (14). However, the data presented here is somewhat at odds with

484 recently published studies investigating the impact of IFI44 (42) and IFI44L (43) on
485 virus in vitro. In the published studies reducing IFI44 or IFI44L in vitro using siRNA
486 led to increased viral recovery, which was hypothesized to be linked to decreased
487 ISG expression. We did not see an effect of IFI44 or IFI44L over-expression on the
488 expression of the ISG Mx1. One possible difference between study designs is the
489 role of cell proliferation. We observed that IFI44 and IFI44L had a significant anti-
490 proliferative effect and to normalise we counted cell numbers in parallel wells prior to
491 infections and altered the viral inoculum to ensure equivalent MOI were used. The
492 parallels between the in vivo and in vitro phenotype give us confidence that the
493 genes can have an antiviral function.

494 One question of interest is about the redundancy of ISGs in the control of infection.
495 Using knockout mouse models, an increase in RSV disease severity has been seen
496 for a variety of antiviral ISGs such as Ifitm3 (44), Ifitm1 (5), and Irf7 (8). It is curious
497 that in these *in vitro* and *in vivo* models, single gene loss can result in the loss of viral
498 control, when the host network of ISGs consists of potentially over 1000 genes.
499 Whilst some associations between individual ISGs and disease severity have been
500 observed in humans – for example IFITM3 (45, 46), more often primary
501 immunodeficiencies caused by mutations in the interferon sensing and signalling
502 pathways such as STAT1 and TLR3 display incomplete penetrance and only specific
503 susceptibilities (47). Potentially the use of large volumes relative to lung size and
504 high doses of virus to ensure infection in the mouse model stresses the system and
505 therefore the role of individual genes becomes more apparent. It was of note that we
506 observed a significant reduction in IFI44 and IFI44L expression associated with
507 infant patients requiring PICU admission, when tested in isolation, but in the global
508 comparison, there were other genes that were more significantly different,

509 suggesting there may be a more coordinated effect that influences disease severity.
510 It should also be noted that the children requiring intensive care were significantly
511 younger, which may impact gene expression. This may be the result of reduced IFN
512 activity as a whole – this has been seen in another cohort of children with RSV
513 infection (48) where those children with severe infection had lower global expression
514 of ISG. This suggests that ISGs work in concert to control infection, targeting
515 different aspects of the viral life cycle, with some factors such as IFITM1 controlling
516 entry (5) and others restricting replication within the cell. Further work is required to
517 understand whether lower expression levels during human infection predispose to
518 severe RSV and might explain some of the heterogeneity in disease severity in
519 children. Several expression quantitative trait loci (eQTL) are described for these
520 genes (49), including one located within the *IFI44L* gene, rs273259, that was the top-
521 hit in a genome-wide association study of adverse responses to a live virus vaccine
522 (MMR) (50). Cells with the rs273259 risk allele expressed *IFI44* at lower levels, and
523 *IFI44L* with altered splice isoform levels (50). These findings establish a precedent
524 for polymorphisms affecting *IFI44* and *IFI44L* expression to influence predisposition
525 to a severe response to viral infection.

526 Our study demonstrates that *IFI44* and *IFI44L* play a role in the control of RSV
527 infection. They work intracellularly, reducing the ability of the virus to replicate. Since
528 the proteins are anti-proliferative, this may be part of the mechanism. Understanding
529 how they reduce viral replication may provide future avenues for therapeutic
530 interventions.

531 **Acknowledgements**

532 Marcus Dorner and Jessie Skelton for providing lentiviral constructs for gene
533 expression. DCB studentship was funded by The Wellcome Trust (109056/Z/15/A).

534 **Contributions**

535 DCB: Conceptualization, Investigation, Methodology, Writing – original draft; DH-C:
536 Formal analysis; SC: Resources, Investigation; CB: Investigation; IB: Resources;
537 MK: Formal analysis, Supervision; JH: Resources; ML: Supervision, Funding
538 Acquisition; JFE: Resources; PK: Supervision, Writing- Review and editing; JST:
539 Conceptualization, Funding Acquisition, Writing – original draft.

540 **Declaration of Interests**

541 The authors declare no competing interests.

542 **References**

- 543 1. Tregoning JS, Schwarze J. 2010. Respiratory viral infections in infants: causes, clinical
544 symptoms, virology, and immunology. *Clin Microbiol Rev* 23:74-98.
- 545 2. Garcia CG, Bhore R, Soriano-Fallas A, Trost M, Chason R, Ramilo O, Mejias A. 2010. Risk
546 factors in children hospitalized with RSV bronchiolitis versus non-RSV bronchiolitis.
547 *Pediatrics* 126:e1453-60.
- 548 3. Murray J, Bottle A, Sharland M, Modi N, Aylin P, Majeed A, Saxena S, Medicines for Neonates
549 Investigator G. 2014. Risk factors for hospital admission with RSV bronchiolitis in England: a
550 population-based birth cohort study. *PLoS One* 9:e89186.
- 551 4. Zhang W, Zhang L, Zan Y, Du N, Yang Y, Tien P. 2015. Human respiratory syncytial virus
552 infection is inhibited by IFN-induced transmembrane proteins. *J Gen Virol* 96:170-82.
- 553 5. Smith SE, Busse DC, Binter S, Weston S, Diaz Soria C, Laksono BM, Clare S, Van Nieuwkoop S,
554 Van den Hoogen BG, Clement M, Marsden M, Humphreys IR, Marsh M, de Swart RL, Wash
555 RS, Tregoning JS, Kellam P. 2019. Interferon-Induced Transmembrane Protein 1 Restricts
556 Replication of Viruses That Enter Cells via the Plasma Membrane. *J Virol* 93.
- 557 6. Subramanian G, Kuzmanovic T, Zhang Y, Peter CB, Veleparambil M, Chakravarti R, Sen GC,
558 Chattopadhyay S. 2018. A new mechanism of interferon's antiviral action: Induction of
559 autophagy, essential for paramyxovirus replication, is inhibited by the interferon stimulated
560 gene, TDRD7. *PLOS Pathogens* 14:e1006877.
- 561 7. Behera AK, Kumar M, Lockey RF, Mohapatra SS. 2002. 2'-5' Oligoadenylate synthetase plays
562 a critical role in interferon-gamma inhibition of respiratory syncytial virus infection of human
563 epithelial cells. *J Biol Chem* 277:25601-8.
- 564 8. McDonald JU, Kafrou M, Clare S, Hale C, Ivanova M, Huntley D, Dorner M, Wright VJ, Levin
565 M, Martinon-Torres F, Herberg JA, Tregoning JS. 2016. A Simple Screening Approach To

- 566 Prioritize Genes for Functional Analysis Identifies a Role for Interferon Regulatory Factor 7 in
567 the Control of Respiratory Syncytial Virus Disease. *mSystems* 1.
- 568 9. Takahashi K, Kitamura N, Shibui T, Kamizono M, Matsui R, Yoshiyama Y, Maeda T, Kondo J,
569 Honda Y, Yamada E, et al. 1990. Cloning, sequencing and expression in *Escherichia coli* of
570 cDNA for a non-A, non-B hepatitis-associated microtubular aggregates protein. *J Gen Virol*
571 71 (Pt 9):2005-11.
- 572 10. Honda Y, Kondo J, Maeda T, Yoshiyama Y, Yamada E, Shimizu YK, Shikata T, Ono Y. 1990.
573 Isolation and purification of a non-A, non-B hepatitis-associated microtubular aggregates
574 protein. *J Gen Virol* 71 (Pt 9):1999-2004.
- 575 11. Carlton-Smith C, Elliott RM. 2012. Viperin, MTAP44, and protein kinase R contribute to the
576 interferon-induced inhibition of Bunyamwera Orthobunyavirus replication. *J Virol* 86:11548-
577 57.
- 578 12. Power D, Santoso N, Dieringer M, Yu J, Huang H, Simpson S, Seth I, Miao H, Zhu J. 2015. IFI44
579 suppresses HIV-1 LTR promoter activity and facilitates its latency. *Virology* 481:142-50.
- 580 13. Hallen LC, Burki Y, Ebeling M, Broger C, Siegrist F, Oroszlan-Szovik K, Bohrmann B, Certa U,
581 Foser S. 2007. Antiproliferative activity of the human IFN-alpha-inducible protein IFI44. *J*
582 *Interferon Cytokine Res* 27:675-80.
- 583 14. Schoggins JW, Wilson SJ, Panis M, Murphy MY, Jones CT, Bieniasz P, Rice CM. 2011. A diverse
584 range of gene products are effectors of the type I interferon antiviral response. *Nature*
585 472:481-5.
- 586 15. Imgenberg-Kreuz J, Sandling JK, Almlof JC, Nordlund J, Signer L, Norheim KB, Omdal R,
587 Ronnblom L, Eloranta ML, Syvanen AC, Nordmark G. 2016. Genome-wide DNA methylation
588 analysis in multiple tissues in primary Sjogren's syndrome reveals regulatory effects at
589 interferon-induced genes. *Annals of the Rheumatic Diseases* 75:2029-2036.
- 590 16. Yeung KS, Chung BHY, Choufani S, Mok MY, Wong WL, Mak CCY, Yang WL, Lee PPW, Wong
591 WHS, Chen YA, Grafodatskaya D, Wong RWS, Lau CS, Chan DTM, Weksberg R, Lau YL. 2017.
592 Genome-Wide DNA Methylation Analysis of Chinese Patients with Systemic Lupus
593 Erythematosus Identified Hypomethylation in Genes Related to the Type I Interferon
594 Pathway. *Plos One* 12.
- 595 17. Zhao M, Zhou Y, Zhu BC, Wan MJ, Jiang TT, Tan QQ, Liu Y, Jiang JQ, Luo SHT, Tan YX, Wu HJ,
596 Renauer P, Gutierrez MDA, Palma MJC, Castro RO, Fernandez-Roldan C, Raya E, Faria R,
597 Carvalho C, Alarcon-Riquelme ME, Xiang ZY, Chen JW, Li F, Ling GH, Zhao HJ, Liao XP, Lin YK,
598 Sawalha AH, Lu QJ. 2016. IFI44L promoter methylation as a blood biomarker for systemic
599 lupus erythematosus. *Annals of the Rheumatic Diseases* 75:1998-2006.
- 600 18. Huang WC, Tung SL, Chen YL, Chen PM, Chu PY. 2018. IFI44L is a novel tumor suppressor in
601 human hepatocellular carcinoma affecting cancer stemness, metastasis, and drug resistance
602 via regulating met/Src signaling pathway. *BMC Cancer* 18:609.
- 603 19. Li H, Wang X, Fang Y, Huo Z, Lu X, Zhan X, Deng X, Peng C, Shen B. 2017. Integrated
604 expression profiles analysis reveals novel predictive biomarker in pancreatic ductal
605 adenocarcinoma. *Oncotarget* doi:10.18632/oncotarget.16732.
- 606 20. Haralambieva IH, Ovsyannikova IG, Kennedy RB, Larrabee BR, Zimmermann MT, Grill DE,
607 Schaid DJ, Poland GA. 2017. Genome-wide associations of CD46 and IFI44L genetic variants
608 with neutralizing antibody response to measles vaccine. *Hum Genet* 136:421-435.
- 609 21. Herberg JA, Kaforou M, Wright VJ, Shailes H, Eleftherohorinou H, Hoggart CJ, Cebey-Lopez
610 M, Carter MJ, Janes VA, Gormley S, Shimizu C, Tremoulet AH, Barendregt AM, Salas A,
611 Kanegaye J, Pollard AJ, Faust SN, Patel S, Kuijpers T, Martinon-Torres F, Burns JC, Coin LJ,
612 Levin M, Consortium I. 2016. Diagnostic Test Accuracy of a 2-Transcript Host RNA Signature
613 for Discriminating Bacterial vs Viral Infection in Febrile Children. *JAMA* 316:835-45.
- 614 22. Barrett T, Wilhite SE, Ledoux P, Evangelista C, Kim IF, Tomaszewsky M, Marshall KA, Phillippy
615 KH, Sherman PM, Holko M, Yefanov A, Lee H, Zhang N, Robertson CL, Serova N, Davis S,

- 616 Soboleva A. 2013. NCBI GEO: archive for functional genomics data sets--update. *Nucleic*
617 *Acids Res* 41:D991-5.
- 618 23. Davis S, Meltzer PS. 2007. GEOquery: a bridge between the Gene Expression Omnibus (GEO)
619 and BioConductor. *Bioinformatics* 23:1846-7.
- 620 24. Team RC. 2018. R: A language and environment for statistical computing. , R Foundation for
621 Statistical Computing, Vienna, Austria, <https://www.R-project.org/>.
- 622 25. Du P, Kibbe WA, Lin SM. 2008. lumi: a pipeline for processing Illumina microarray.
623 *Bioinformatics* 24:1547-8.
- 624 26. Hallak LK, Spillmann D, Collins PL, Peeples ME. 2000. Glycosaminoglycan sulfation
625 requirements for respiratory syncytial virus infection. *J Virol* 74:10508-13.
- 626 27. Livak KJ, Schmittgen TD. 2001. Analysis of relative gene expression data using real-time
627 quantitative PCR and the 2^{-Delta Delta C(T)} Method. *Methods* 25:402-8.
- 628 28. Sanjana NE, Shalem O, Zhang F. 2014. Improved vectors and genome-wide libraries for
629 CRISPR screening. *Nat Methods* 11:783-4.
- 630 29. Sievers F, Wilm A, Dineen D, Gibson TJ, Karplus K, Li WZ, Lopez R, McWilliam H, Remmert M,
631 Soding J, Thompson JD, Higgins DG. 2011. Fast, scalable generation of high-quality protein
632 multiple sequence alignments using Clustal Omega. *Molecular Systems Biology* 7.
- 633 30. Richard CA, Rincheval V, Lassoued S, Fix J, Cardone C, Esneau C, Nekhai S, Galloux M,
634 Rameix-Welti MA, Sizun C, Eleouet JF. 2018. RSV hijacks cellular protein phosphatase 1 to
635 regulate M2-1 phosphorylation and viral transcription. *PLoS Pathog* 14:e1006920.
- 636 31. Skarnes WC, Rosen B, West AP, Koutsourakis M, Bushell W, Iyer V, Mujica AO, Thomas M,
637 Harrow J, Cox T, Jackson D, Severin J, Biggs P, Fu J, Nefedov M, de Jong PJ, Stewart AF,
638 Bradley A. 2011. A conditional knockout resource for the genome-wide study of mouse gene
639 function. *Nature* 474:337-42.
- 640 32. Daumke O, Praefcke GJ. 2016. Invited review: Mechanisms of GTP hydrolysis and
641 conformational transitions in the dynamin superfamily. *Biopolymers* 105:580-93.
- 642 33. McDowell IC, Modak TH, Lane CE, Gomez-Chiarri M. 2016. Multi-species protein similarity
643 clustering reveals novel expanded immune gene families in the eastern oyster *Crassostrea*
644 *virginica*. *Fish Shellfish Immunol* 53:13-23.
- 645 34. Praefcke GJ, Kloep S, Benschaid U, Lilie H, Prakash B, Herrmann C. 2004. Identification of
646 residues in the human guanylate-binding protein 1 critical for nucleotide binding and
647 cooperative GTP hydrolysis. *J Mol Biol* 344:257-69.
- 648 35. Garcia MA, Gil J, Ventoso I, Guerra S, Domingo E, Rivas C, Esteban M. 2006. Impact of
649 protein kinase PKR in cell biology: from antiviral to antiproliferative action. *Microbiol Mol*
650 *Biol Rev* 70:1032-60.
- 651 36. Wong MT, Chen SS. 2016. Emerging roles of interferon-stimulated genes in the innate
652 immune response to hepatitis C virus infection. *Cell Mol Immunol* 13:11-35.
- 653 37. Gibbs JD, Ornoff DM, Igo HA, Zeng JY, Imani F. 2009. Cell Cycle Arrest by Transforming
654 Growth Factor beta 1 Enhances Replication of Respiratory Syncytial Virus in Lung Epithelial
655 Cells. *Journal of Virology* 83:12424-12431.
- 656 38. Bian T, Gibbs JD, Orvell C, Imani F. 2012. Respiratory syncytial virus matrix protein induces
657 lung epithelial cell cycle arrest through a p53 dependent pathway. *PLoS One* 7:e38052.
- 658 39. Gibbs JD, Ornoff DM, Igo HA, Zeng JY, Imani F. 2009. Cell cycle arrest by transforming growth
659 factor beta1 enhances replication of respiratory syncytial virus in lung epithelial cells. *J Virol*
660 83:12424-31.
- 661 40. Russell RF, McDonald JU, Ivanova M, Zhong Z, Bukreyev A, Tregoning JS. 2015. Partial
662 Attenuation of Respiratory Syncytial Virus with a Deletion of a Small Hydrophobic Gene Is
663 Associated with Elevated Interleukin-1beta Responses. *J Virol* 89:8974-81.
- 664 41. Groves HT, Higham SL, Moffatt MF, Cox MJ, Tregoning JS. 2020. Respiratory Viral Infection
665 Alters the Gut Microbiota by Inducing Inappetence. *mBio* 11:e03236-19.

- 666 42. DeDiego ML, Nogales A, Martinez-Sobrido L, Topham DJ. 2019. Interferon-Induced Protein
667 44 Interacts with Cellular FK506-Binding Protein 5, Negatively Regulates Host Antiviral
668 Responses, and Supports Virus Replication. *MBio* 10.
- 669 43. DeDiego ML, Martinez-Sobrido L, Topham DJ. 2019. NOVEL FUNCTIONS OF THE
670 INTERFERON-INDUCED PROTEIN 44-LIKE (IFI44L) AS A FEEDBACK REGULATOR OF HOST
671 ANTIVIRAL RESPONSES. *J Virol* doi:10.1128/jvi.01159-19.
- 672 44. Everitt AR, Clare S, McDonald JU, Kane L, Harcourt K, Ahras M, Lall A, Hale C, Rodgers A,
673 Young DB, Haque A, Billker O, Tregoning JS, Dougan G, Kellam P. 2013. Defining the Range of
674 Pathogens Susceptible to Ifitm3 Restriction Using a Knockout Mouse Model. *Plos One* 8.
- 675 45. Zhang YH, Zhao Y, Li N, Peng YC, Giannoulatou E, Jin RH, Yan HP, Wu H, Liu JH, Liu N, Wang
676 DY, Shu YL, Ho LP, Kellam P, McMichael A, Dong T. 2013. Interferon-induced transmembrane
677 protein-3 genetic variant rs12252-C is associated with severe influenza in Chinese
678 individuals. *Nat Commun* 4:1418.
- 679 46. Everitt AR, Clare S, Pertel T, John SP, Wash RS, Smith SE, Chin CR, Feeley EM, Sims JS, Adams
680 DJ, Wise HM, Kane L, Goulding D, Digard P, Anttila V, Baillie JK, Walsh TS, Hume DA, Palotie
681 A, Xue Y, Colonna V, Tyler-Smith C, Dunning J, Gordon SB, Gen II, Investigators M, Smyth RL,
682 Openshaw PJ, Dougan G, Brass AL, Kellam P. 2012. IFITM3 restricts the morbidity and
683 mortality associated with influenza. *Nature* 484:519-23.
- 684 47. Casanova JL, Abel L. 2018. Human genetics of infectious diseases: Unique insights into
685 immunological redundancy. *Seminars in Immunology* 36:1-12.
- 686 48. Thwaites RS, Coates M, Ito K, Ghazaly M, Feather C, Abdulla F, Tunstall T, Jain P, Cass L,
687 Rapeport G, Hansel TT, Nadel S, Openshaw P. 2018. Reduced Nasal Viral Load and IFN
688 Responses in Infants with Respiratory Syncytial Virus Bronchiolitis and Respiratory Failure.
689 *Am J Respir Crit Care Med* 198:1074-1084.
- 690 49. Westra HJ, Peters MJ, Esko T, Yaghootkar H, Schurmann C, Kettunen J, Christiansen MW,
691 Fairfax BP, Schramm K, Powell JE, Zhernakova A, Zhernakova DV, Veldink JH, Van den Berg
692 LH, Karjalainen J, Withoff S, Uitterlinden AG, Hofman A, Rivadeneira F, 't Hoen PAC, Reinmaa
693 E, Fischer K, Nelis M, Milani L, Melzer D, Ferrucci L, Singleton AB, Hernandez DG, Nalls MA,
694 Homuth G, Nauck M, Radke D, Volker U, Perola M, Salomaa V, Brody J, Suchy-Dicey A,
695 Gharib SA, Enquobahrie DA, Lumley T, Montgomery GW, Makino S, Prokisch H, Herder C,
696 Roden M, Grallert H, Meitinger T, Strauch K, Li Y, Jansen RC, et al. 2013. Systematic
697 identification of trans eQTLs as putative drivers of known disease associations. *Nature*
698 *Genetics* 45:1238-U195.
- 699 50. Feenstra B, Pasternak B, Geller F, Carstensen L, Wang T, Huang F, Eitson JL, Hollegaard MV,
700 Svanstrom H, Vestergaard M, Hougaard DM, Schoggins JW, Jan LY, Melbye M, Hviid A. 2014.
701 Common variants associated with general and MMR vaccine-related febrile seizures. *Nat*
702 *Genet* 46:1274-82.

703

704 **Figure Titles and Legends**

705 **Figure 1. IFI44 and IFI44L mRNA levels are reduced in the blood of infants with**
706 **severe RSV infection. (a)** Demographic and clinical features of patient groups.
707 Patients were febrile children with immunofluorescence-confirmed RSV infection.
708 Patients with suspected or confirmed bacterial co-infection were excluded (n = 4). **(b)**
709 IFI44 or **(c)** IFI44L mRNA expression levels, measured in blood PBMC by microarray
710 in either patients admitted to a general ward with mild RSV illness or admitted to a
711 paediatric intensive care unit (PICU) at the same hospital. * P < 0.05, ** P < 0.01.
712 Significance by unpaired t-test. **(d)** Pearson correlation analysis of expression of
713 IFI44 and IFI44L. P < 0.001. **(e)** Volcano plot of fold change in gene expression by
714 microarray between general hospital and intensive care admission.

715 **Figure 2. IFI44 and IFI44L are IFN-I responsive genes upregulated during RSV**
716 **infection. (a)** *IFI44* and *IFI44L* mRNA expression in A549 cells treated with 500 IU
717 ml⁻¹ IFN α 2a or **(b)** infected with RSV A2 (m.o.i. 0.1) for 2-24 hours. N \geq 3. **(c)** IFI44
718 and IFI44L protein levels in A549 cells treated with 0-1000 IU ml⁻¹ IFN α 2a for 24 or
719 48 hours. **(d)** RSV L gene copies in RSV infected A549 cells as for **b**. **(e)** A549 cells
720 treated with IFN α 2a for 16 hours prior to infection with RSV A2 (m.o.i. 0.1) for 24
721 hours. Viral RNA relative to untreated controls. N=3. **(f)** 8-10-week-old BALB/c mice
722 were infected intranasally with 2 x 10⁵ pfu RSV A2. Change in expression of *Ifi44*
723 and *Ifi44l* mRNA in infected mice relative to mice given PBS intranasally at the time
724 of infection. **(g)** Total L gene copy number per μ g RNA from whole lung tissue. N \geq 4
725 animals per group at each time point. Data are presented as the mean +/- SEM.
726 Significance relative to untreated controls (**a-b, e**), PBS-treated (**f**), or noted groups
727 (**d, g**) assessed by ANOVA. * P < 0.05, ** P < 0.01, *** P < 0.001, **** P < 0.0001.

728 **Figure 3. Overexpression of IFI44 or IFI44L reduces RSV infection. (a)** *IFI44*,
729 *IFI44L*, and *Mx1* mRNA levels relative to *GAPDH* in stably transduced monoclonal
730 A549 cells lines. Cells were cultured in normal growth medium or medium
731 supplemented with 500 IU ml⁻¹ IFN α 2a for 24 hours. **(b)** Stably transduced cell lines
732 were infected with rgRSV (m.o.i. 0.1 or 0.01) and infection assessed by flow
733 cytometry after 24 hours. Representative experiment showing GFP⁺ population of
734 single RFP⁺ cells. **(c)** RSV infection of stably transduced cell lines relative to the
735 Vector control. N \geq 5. **(d)** RSV L gene 24 hours post-infection with wild-type RSV A2
736 relative to Vector control. **(e)** Viral titre (WT RSV A2) relative to Vector control in cell
737 supernatant at 48 hpi by plaque assay. **(f)** A549 cells were transduced with either
738 FLUC (Vector) or IFI44 lentivirus and expression of IFI44 detected by Western
739 blotting after 48 hours. **(g)** Transduced A549 cells were infected with rgRSV (m.o.i.
740 0.8) after 24 hours, and infectivity of transduced (RFP⁺) cells assessed 24 hours
741 after infection. N=3. Individual points represent the result of an independent
742 experiment. Bars show the mean +/- SEM. * represents significance relative to cells
743 transduced with empty vector, assessed by ANOVA **(a)** or ratio paired t-test **(c-e)**.
744 Analysis was done prior to data transformation. * P < 0.05, ** P < 0.01, *** P < 0.001,
745 **** P < 0.0001.

746 **Figure 4. Loss of IFI44 or IFI44L enhances RSV infection *in vitro*. (a)** *IFI44* and
747 *IFI44L* mRNA expression after transfection with 50 nM esiRNA-IFI44 or a non-
748 targeting esiRNA control (NT). 24 hours after transfection cells were treated with 500
749 IU ml⁻¹ IFN α 2a for 16 hours prior to infection with RSV A2 (m.o.i. 0.1) for 48 hours.
750 N=3. **(b)** L gene copy number assessed 48 hours after infection and shown relative
751 to the NT control. N=5. **(c)** A549 monoclonal knockout cell lines were generated
752 through CRISPR-Cas9 gene editing. IFI44 or IFI44L protein in wild-type cells treated

753 with IFN α 2a or monoclonal CRISPR-Cas9 edited A549 cells. **(d)** Cells were treated
754 with 500 IU ml⁻¹ IFN α 2a 16 hours prior to infection with RSV A2 (m.o.i. 0.1 or 0.01)
755 for 24 hours. RSV L gene copy number shown relative to the WT control. N=3. **(e)**
756 Knockout cell lines were pre-treated with IFN α 2a as for **c** and subsequently infected
757 with RSV A2 (m.o.i. 0.1) for 48 hours. Viral titre in cell supernatant relative to the WT
758 control. N=3. Points represent a single independent experiment with a bar at the
759 mean +/- SEM. Significance relative to the WT or NT controls by ratio paired T test.
760 Analysis was done prior to data transformation. * P < 0.05, ** P < 0.01. ns = not
761 significant.

762 **Figure 5. IFI44 and IFI44L are anti-proliferative.** A549 monoclonal knockout cell
763 lines were seeded at equal densities and viable cell number quantified after 6-48
764 hours using a colorimetric metabolic activity assay **(a)** or by trypan blue exclusion (#
765 P < 0.05 between Δ IFI44L and vector). **(b)**. A549 stably transduced monoclonal cell
766 lines expressing IFI44, IFI44L, or transduced with empty vector were seeded at
767 equal densities and viable cell number quantified 24 hours later by colorimetric
768 metabolic activity assay **(c)** or after 6-48h by trypan blue exclusion **(d)** (* P <0.05,
769 **** P < 0.0001 between IFI44 and vector, # P <0.05, ## P <0.01 between IFI44L and
770 vector) N \geq 3. **(e)** Representative histograms of stably transduced A549 cell lines
771 treated with CellTrace Violet and allowed to proliferate for 72 hours before analysis
772 by flow cytometry. WT cells were stained or treated with vehicle only and
773 immediately fixed prior to analysis for positive (red) and negative (grey) controls. **(f)**
774 Mean fluorescence intensity (MFI) of cell trace violet quantified relative to Vector
775 control over three independent repeats. Cytotoxicity was assessed by LDH release
776 assay 24-48 hours after plating in overexpression **(g)** or knockout cells **(h)**. N=3.
777 Significance to WT or Vector controls assessed by ratio paired T test prior to data

778 transformation. Points represent a single independent experiment with a bar at the
779 mean +/- SEM. * P < 0.05, ** < P < 0.01, *** P < 0.001, **** P < 0.0001 in panels a, c
780 and f between indicated bar and vector.

781

782 **Figure 6. IFI44 and IFI44L reduce RSV polymerase activity and restrict**
783 **infection independent of GTP-binding. (a)** Stably transduced A549 cells were
784 infected with rgRSV (m.o.i. 0.1) for 8 hours and infectivity assessed by measuring
785 the percentage of RFP⁺ single cells that were GFP⁺. Representative dot plot from a
786 single independent experiment. Population shown was gated for single RFP⁺ cells.
787 **(b)** Quantification of rgRSV infection relative to Vector transduced control as
788 described in **a**. N=3. **(c)** Stably transduced A549 cell lines were incubated with RSV
789 A2 (m.o.i. 2) for 1 hour at 4 °C then harvested for analysis of RSV L gene copy
790 number. N=3. **(d)** Stably transduced 293T cell lines were transfected with pSV-β-Gal,
791 pCAGGS-T7, the pGEM3-Gaussia/Firefly minigenome and plasmids encoding RSV
792 M2-1, P, L, and N. 24 hours later FLUC activity was assessed and normalised to the
793 negative control and β-Galactosidase expression levels. Normalised FLUC activity
794 shown relative to polyclonal parental 293T cells (WT). N=3. **(e)** ClustalW multiple
795 sequence alignment of human IFI44 and IFI44L. Four sections were selected to
796 show the residues predicted to be essential for GTP binding and GTPase function
797 (highlighted by a red box). Consensus sequence for each G1-G4 region shown
798 below. **(f)** A549 cells were transduced with 2×10^5 TU lentivirus expressing either WT
799 IFI44, IFI44Δ193-201 (G1 region deleted), or FLUC (Vector). 24 hours later cells
800 were infected with rgRSV (m.o.i. 0.8) and infectivity assessed as for **a** 24 hours after
801 infection. N=3. Significance to Vector transduced or WT controls assessed by ratio
802 paired t-test prior to data transformation. Points represent a single independent

803 experiment with a bar at the mean +/- SEM * P < 0.05, ** < P < 0.01. ns = not
804 significant.

805 **Figure 7. RSV infection severity is enhanced in an *Ifi44*^{-/-} mouse model. (a)**

806 Wildtype or *Ifi44*^{-/-} C57BL/6N mice were infected intranasally with 1 x 10⁵ pfu RSV

807 A2. Weight loss was monitored for 7 days. **(b)** BALF and **(c)** lung cell counts. **(d)**

808 Viral load assessed by RSV L gene qPCR. **(e)** IL-6 and IL-1β levels at day 4 post-

809 infection measured by ELISA. Volcano plot of inflammatory cytokines at day 4 **(f)** and

810 day 7 **(g)** by multiplex ELISA. **(g)** *Ifnβ* and **(h)** *Ifnγ* mRNA relative to *Gapdh* (2^{-ΔCt}).

811 Box plots show a line at the median and box edges from the 25th to 75th percentiles,

812 with whiskers from the 5th to 95th percentiles (Prism). N≥4 animals at each time

813 point. Two independent experiments. Significance by ANOVA **(a-e, h-i)** or Student's t-

814 test **(f-g)**. * P < 0.05, ** 0.01, *** P < 0.001.

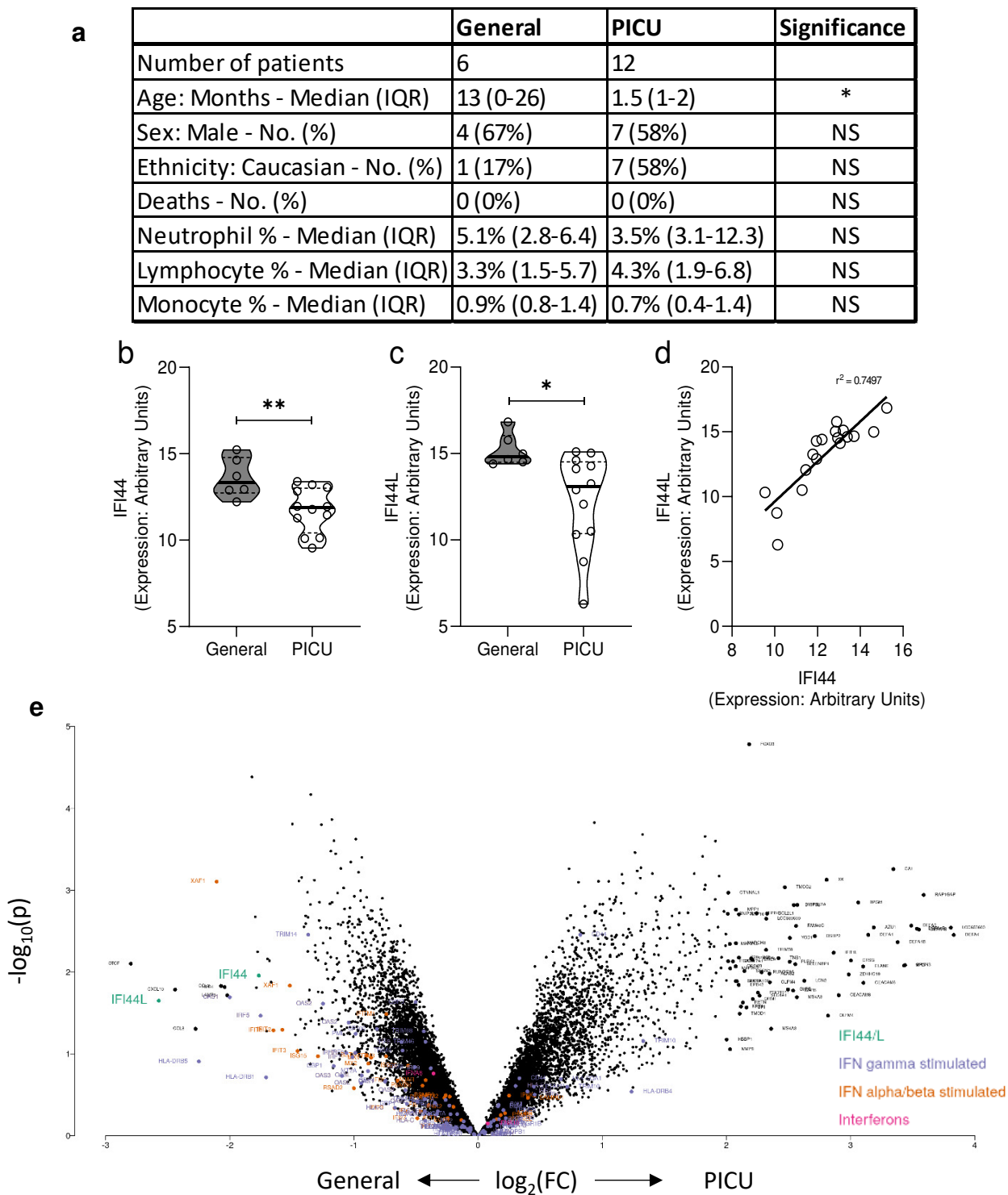


Figure 1. IFI44 and IFI44L mRNA levels are reduced in the blood of infants with severe RSV infection. (a) Demographic and clinical features of patient groups. Patients were febrile children with immunofluorescence-confirmed RSV infection. Patients with suspected or confirmed bacterial co-infection were excluded ($n = 4$). **(b)** IFI44 or **(c)** IFI44L RNA expression levels, measured by in blood PBMC by microarray in either patients admitted to a general ward with mild RSV illness or admitted to a paediatric intensive care unit (PICU) at the same hospital. * $P < 0.05$, ** $P < 0.01$. Significance by unpaired t-test. **(d)** Pearson correlation analysis of expression of IFI44 and IFI44L. $P < 0.001$. **(e)** Volcano plot of fold change in gene expression by microarray between general hospital and intensive care admission.

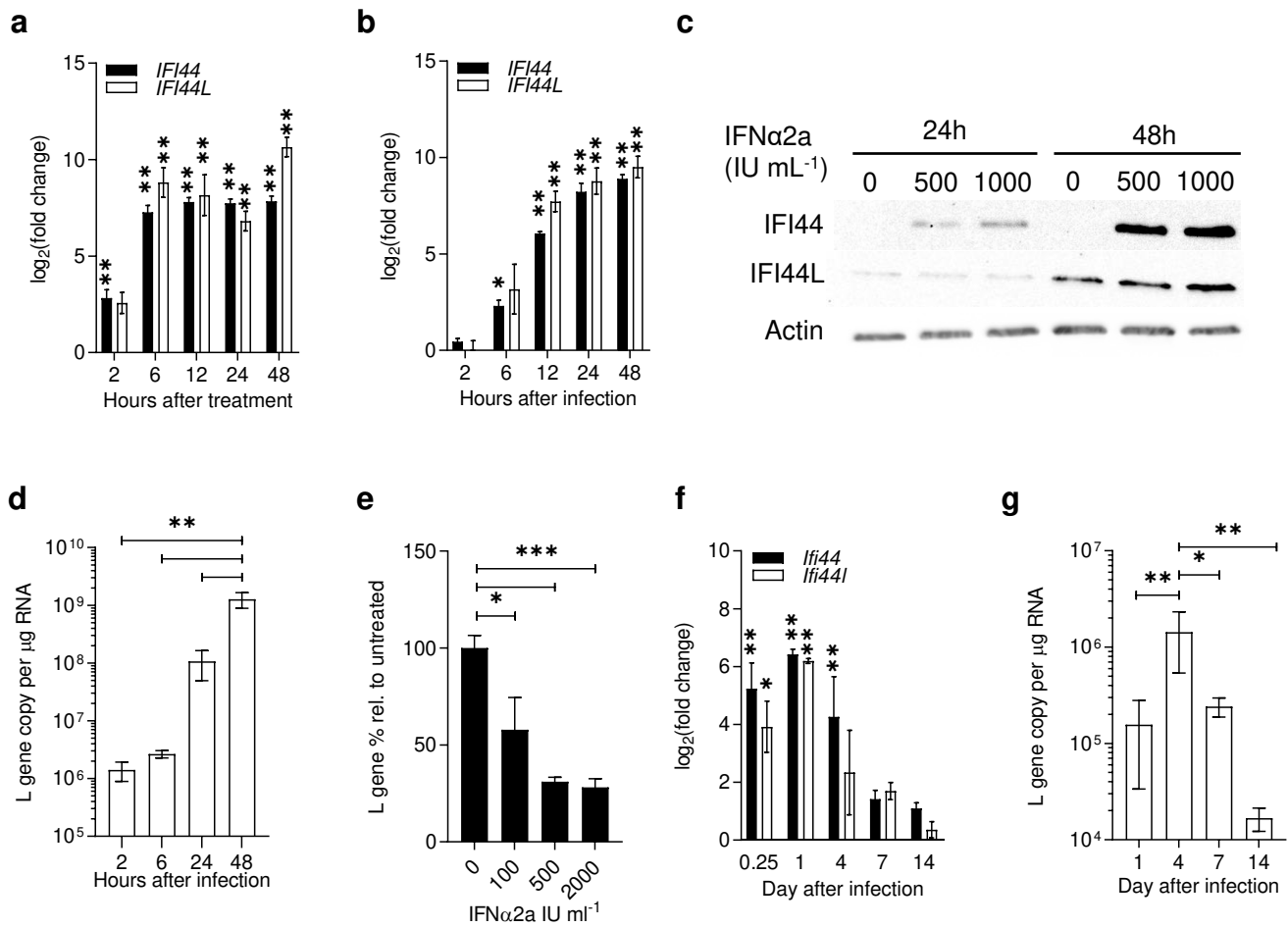


Figure 2. *IFI44* and *IFI44L* are IFN-I responsive genes upregulated during RSV infection.

(a) *IFI44* and *IFI44L* mRNA expression in A549 cells treated with 500 IU mL⁻¹ IFNα2a or (b) infected with RSV A2 (m.o.i. 0.1) for 2-24 hours. N≥3. (c) *IFI44* and *IFI44L* protein levels in A549 cells treated with 0-1000 IU mL⁻¹ IFNα2a for 24 or 48 hours. (d) RSV L gene copies in RSV infected A549 cells as for b. N≥3. (e) A549 cells treated with IFNα2a for 16 hours prior to infection with RSV A2 (m.o.i. 0.1) for 24 hours. Viral RNA relative to untreated controls. N=3. (f) 8-10 week old BALB/c mice were infected intranasally with 2 × 10⁵ pfu RSV A2. Change in expression of *Ifi44* and *Ifi44l* mRNA in infected mice relative to mice given PBS intranasally at the time of infection. (g) Total L gene copy number per μg RNA from whole lung tissue. N≥4 animals per group at each time point. Data are presented as the mean ± SEM. Significance relative to untreated controls (a, b, e), PBS-treated (f), or noted groups (d, g) assessed by ANOVA. * P < 0.05, ** P < 0.01, *** P < 0.001.

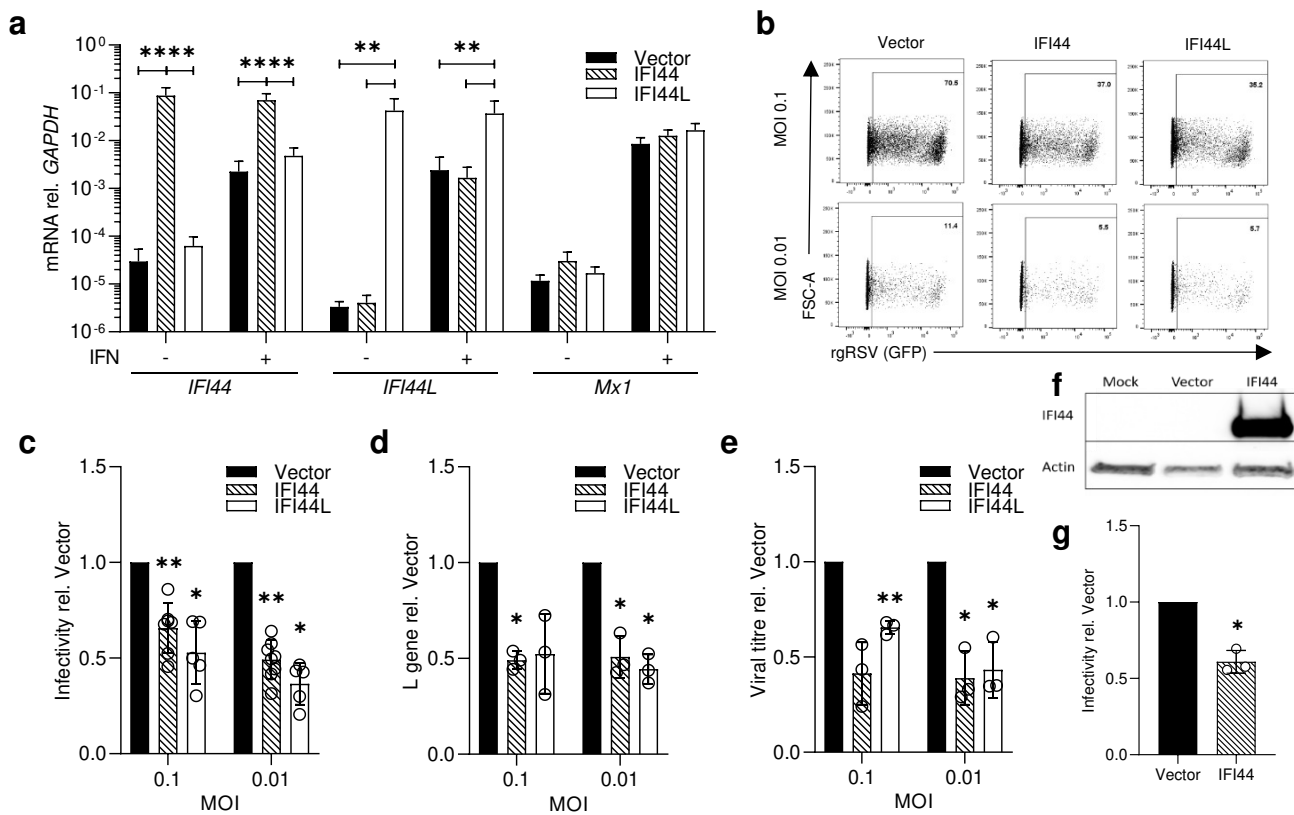


Figure 3. Overexpression of IFI44 or IFI44L reduces RSV infection. (a) *IFI44*, *IFI44L*, and *Mx1* mRNA levels relative to *GAPDH* in stably transduced overexpressing monoclonal A549 cells lines. Cells were cultured in normal growth medium or medium supplemented with 500 IU mL⁻¹ IFN α 2a for 24 hours. (b) Stably transduced cell lines were infected with rgRSV (m.o.i. 0.1 or 0.01) and infectivity assessed by flow cytometry after 24 hours. Representative experiment showing GFP⁺ population of single RFP⁺ cells. (c) RSV infection of stably transduced cell lines relative to the Vector control. N \geq 5. (d) RSV L gene 24 hours post-infection with wild-type RSV A2 relative to Vector control. (e) Viral titre (WT RSV A2) relative to Vector control in cell supernatant at 48 hpi by plaque assay. (f) A549 cells were transduced with either FLUC (Vector) or IFI44 lentivirus and expression of IFI44 detected by Western blotting after 48 hours. (g) Transduced A549 cells were infected with rgRSV (m.o.i. 0.8) after 24 hours, and infectivity of transduced (RFP⁺) cells assessed 24 hours after infection. N=3. Individual points represent the result of an independent experiment. Bars show the mean \pm SEM. * represents significance relative to cells transduced with empty vector, assessed by ANOVA (a) or ratio paired T test (c-e). Analysis was done prior to data transformation. * P < 0.05, ** P < 0.01, *** P < 0.001, **** P < 0.0001.

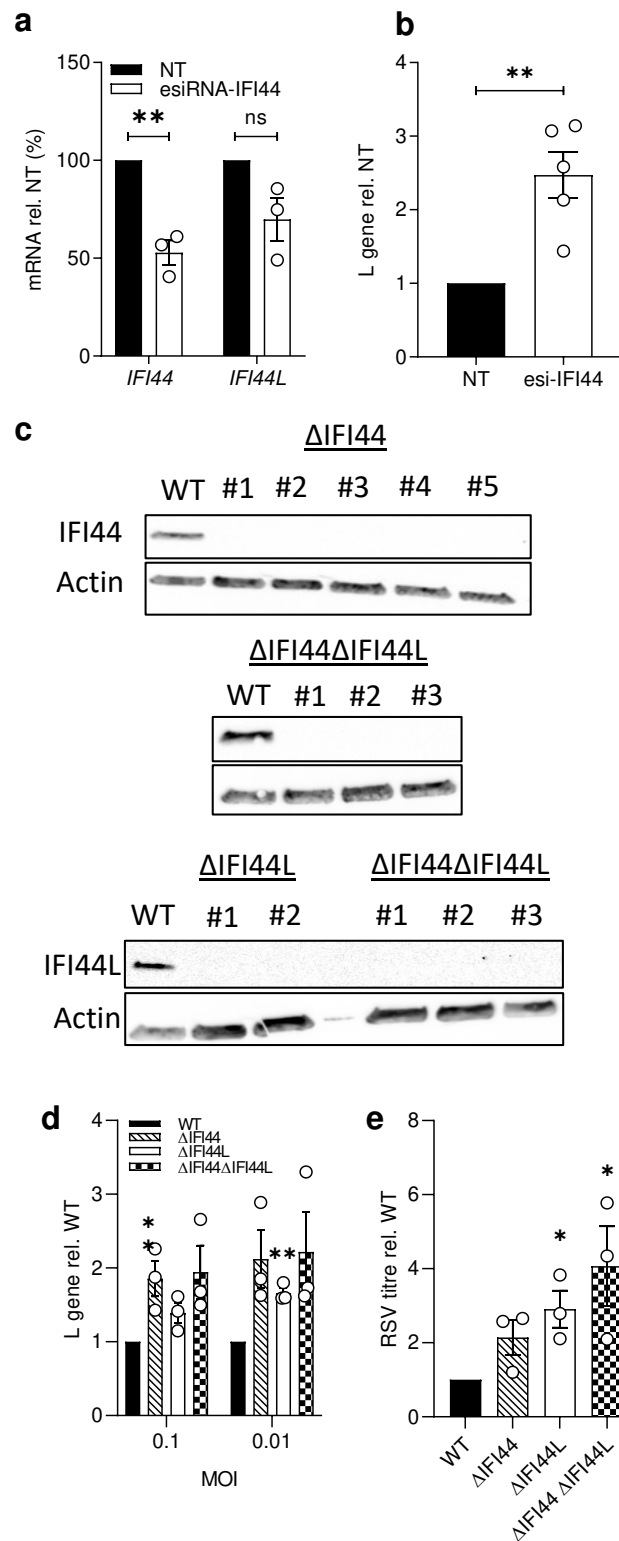


Figure 4. Loss of IFI44 expression enhances RSV infection *in vitro*. (a) *IFI44* and *IFI44L* mRNA expression after transfection with 50 nM esiRNA-IFI44 or a non-targeting esiRNA control (NT). 24 hours after transfection cells were treated with 500 IU mL⁻¹ IFN α 2a for 16 hours prior to infection with RSV A2 (m.o.i. 0.1) for 48 hours. N=3. (b) L gene copy number assessed 48 hours after infection and shown relative to the NT control. N=5. (c) A549 monoclonal knockout cell lines were generated through CRISPR-Cas9 gene editing. IFI44 or IFI44L protein in wild-type cells treated with IFN α 2a or monoclonal CRISPR-Cas9 edited A549 cells. (d) Cells were treated with 500 IU mL⁻¹ IFN α 2a 16 hours prior to infection with RSV A2 (m.o.i. 0.1 or 0.01) for 24 hours. RSV L gene copy number shown relative to the WT control. N=3. (e) Knockout cell lines were pre-treated with IFN α 2a as for c and subsequently infected with RSV A2 (m.o.i. 0.1) for 48 hours. Viral titre in cell supernatant relative to the WT control. N=3. Points represent a single independent experiment with a bar at the mean +/- SEM. Significance relative to the WT or NT controls by ratio paired T test. Analysis was done prior to data transformation. * P < 0.05, ** P < 0.01. ns = not significant.

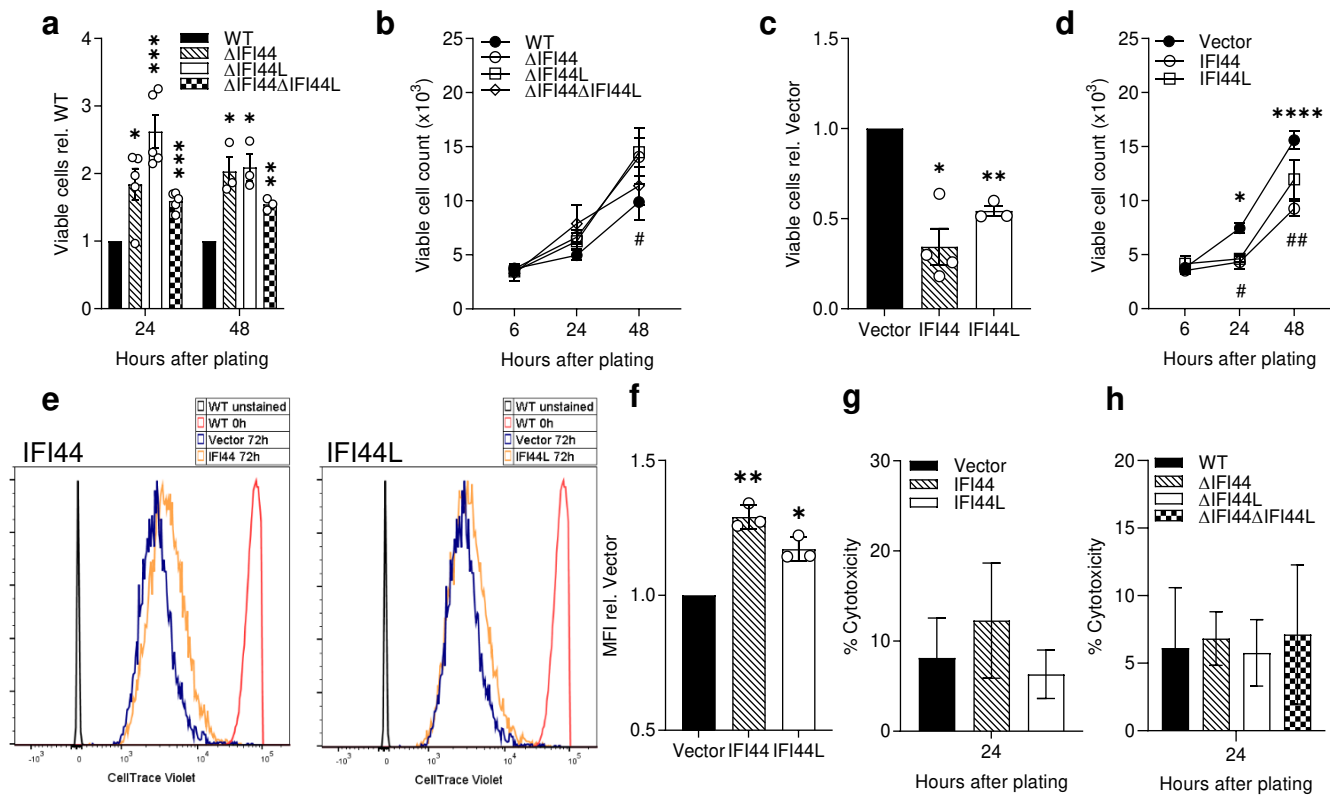


Figure 5. IFI44 and IFI44L are anti-proliferative. A549 monoclonal knockout cell lines were seeded at equal densities and viable cell number quantified after 6-48 hours using a colorimetric metabolic activity assay (**a**) or by trypan blue exclusion (# $P < 0.05$ between Δ IFI44L and vector). (**b**). A549 stably transduced monoclonal cell lines expressing IFI44, IFI44L, or transduced with empty vector were seeded at equal densities and viable cell number quantified 24 hours later by colorimetric metabolic activity assay (**c**) or after 6-48h by trypan blue exclusion (**d**) (* $P < 0.05$, **** $P < 0.0001$ between IFI44 and vector, # $P < 0.05$, ## $P < 0.01$ between IFI44L and vector) $N \geq 3$. (**e**) Representative histograms of stably transduced A549 cell lines treated with CellTrace Violet and allowed to proliferate for 72 hours before analysis by flow cytometry. WT cells were stained or treated with vehicle only and immediately fixed prior to analysis for positive (red) and negative (grey) controls. (**f**) Mean fluorescence intensity (MFI) of cell trace violet quantified relative to Vector control over three independent repeats. Cytotoxicity was assessed by LDH release assay 24-48 hours after plating in overexpression (**g**) or knockout cells (**h**). $N = 3$. Significance to WT or Vector controls assessed by ratio paired T test prior to data transformation. Points represent a single independent experiment with a bar at the mean \pm SEM. * $P < 0.05$, ** $P < 0.01$, *** $P < 0.001$, **** $P < 0.0001$ in panels a, c and f between indicated bar and vector.

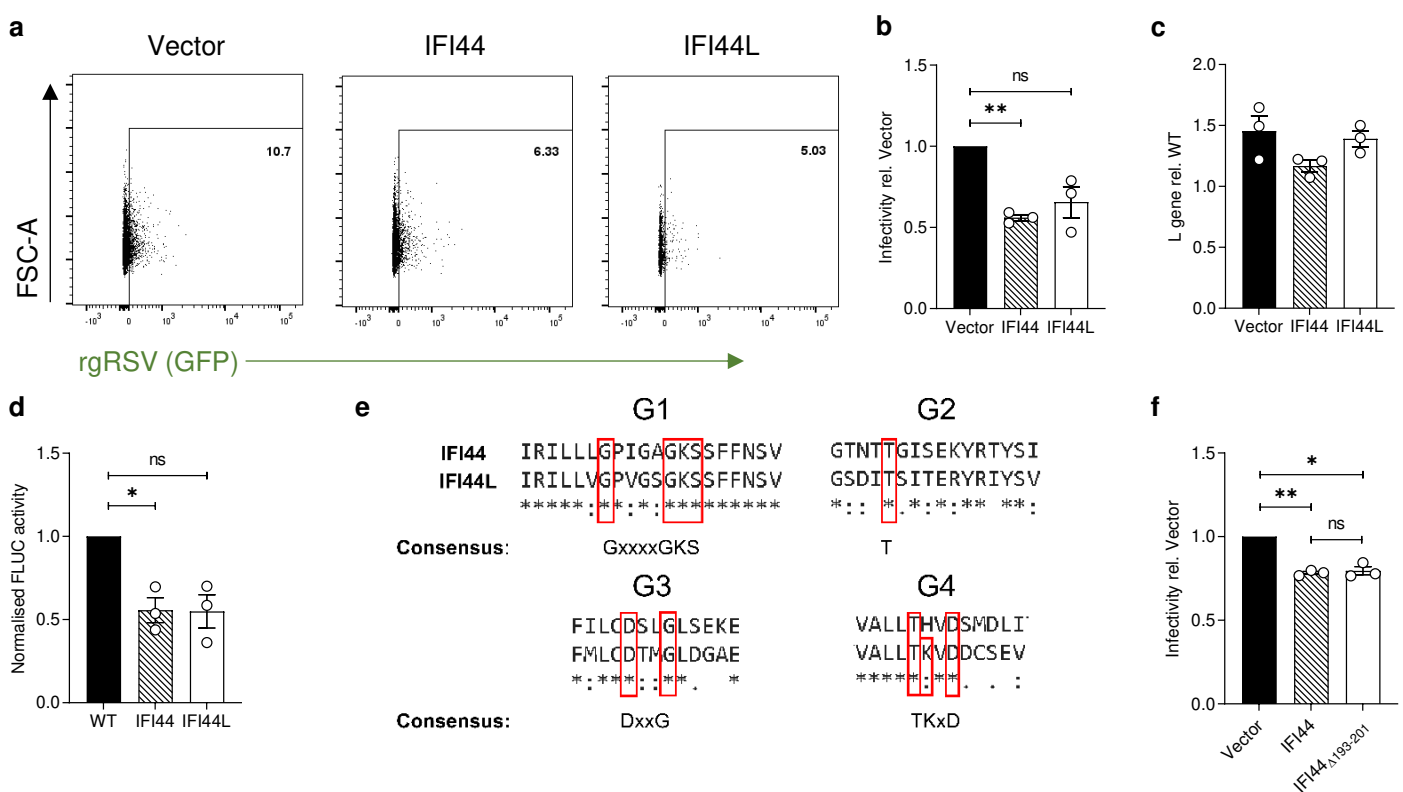


Figure 6. IFI44 and IFI44L reduce RSV polymerase activity and restrict infection independent of GTP-binding. (a) Stably transduced A549 cells were infected with rgRSV (m.o.i. 0.1) for 8 hours and infectivity assessed by measuring the percentage of RFP+ single cells that were GFP+. Representative dot plot from a single independent experiment. Population shown was gated for single RFP+ cells. (b) Quantification of rgRSV infection relative to Vector transduced control as described in a. N=3. (c) Stably transduced A549 cell lines were incubated with RSV A2 (m.o.i. 2) for 1 hour at 4 °C then harvested for analysis of RSV L gene copy number. N=3. (d) Stably transduced 293T cell lines were transfected with pSV- β -Gal, pCAGGS-T7, the pGEM3-Gaussia/Firefly minigenome and plasmids encoding RSV M2-1, P, L, and N. 24 hours later FLUC activity was assessed and normalised to the negative control and β -Galactosidase expression levels. Normalised FLUC activity shown relative to polyclonal parental 293T cells (WT). N=3. (e) ClustalW multiple sequence alignment of human IFI44 and IFI44L. Four sections were selected to show the residues predicted to be essential for GTP binding and GTPase function (highlighted by a red box). Consensus sequence for each G1-G4 region shown below. (f) A549 cells were transduced with 2×10^5 TU lentivirus expressing either WT IFI44, IFI44 Δ 193-201 (G1 region deleted), or FLUC (Vector). 24 hours later cells were infected with rgRSV (m.o.i. 0.8) and infectivity assessed as for a 24 hours after infection. N=3. Significance to Vector transduced or WT controls assessed by ratio paired T test prior to data transformation. Points represent a single independent experiment with a bar at the mean \pm SEM * $P < 0.05$, ** $P < 0.01$. ns = not significant.

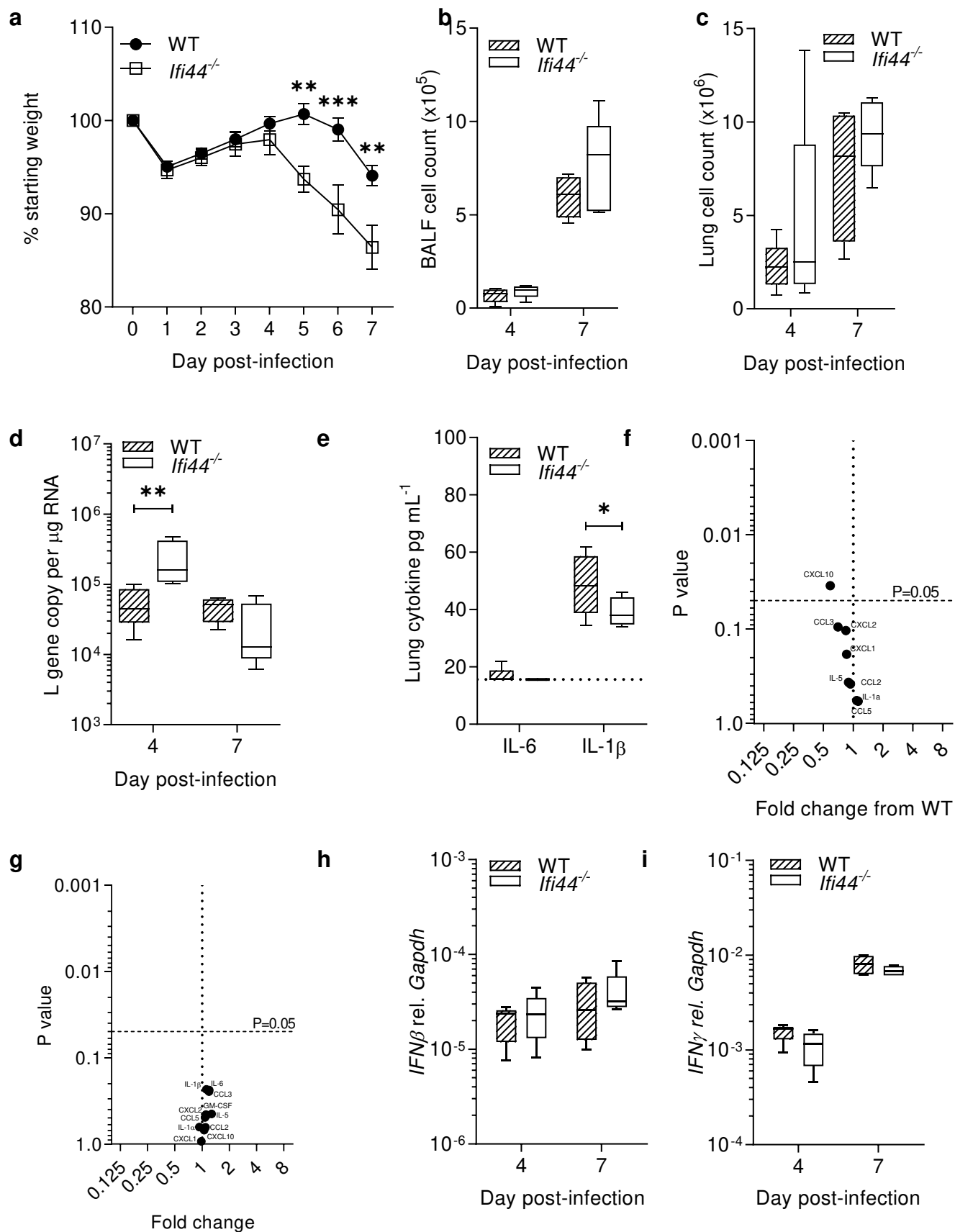


Figure 7. RSV infection severity is enhanced in a *lfi44*^{-/-} mouse model. (a) Wildtype or *lfi44*^{-/-} C57BL/6N mice were infected intranasally with 1 x 10⁵ pfu RSV A2. Weight loss was monitored for 7 days. (b) BALF and (c) lung cell counts. (d) Viral load assessed by RSV L gene qPCR. (e) IL-6 and IL-1β levels at day 4 post-infection measured by ELISA. Volcano plot of inflammatory cytokines at day 4 (f) and day 7 (g) by multiplex ELISA. (h) *IFNβ* and (i) *IFNγ* mRNA relative to *Gapdh* (2^{-ΔCt}). Box plots show a line at the median and box edges from the 25th to 75th percentiles, with whiskers from the 5th to 95th percentiles (Prism). N≥4 animals at each time point. Two independent experiments. Significance by ANOVA (a-e, h-i) or Student's T test (f-g). * P < 0.05, ** 0.01, *** P < 0.001.